



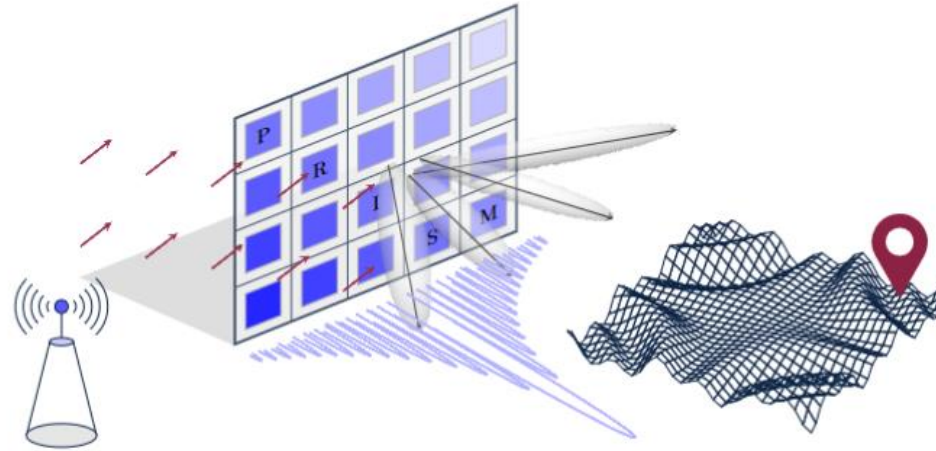
UNIVERSITY OF  
**PATRAS**  
ΠΑΝΕΠΙΣΤΗΜΙΟ ΠΑΤΡΩΝ



HELLENIC REPUBLIC  
National and Kapodistrian  
University of Athens



**ADVEOS**  
A **BEKEN** COMPANY

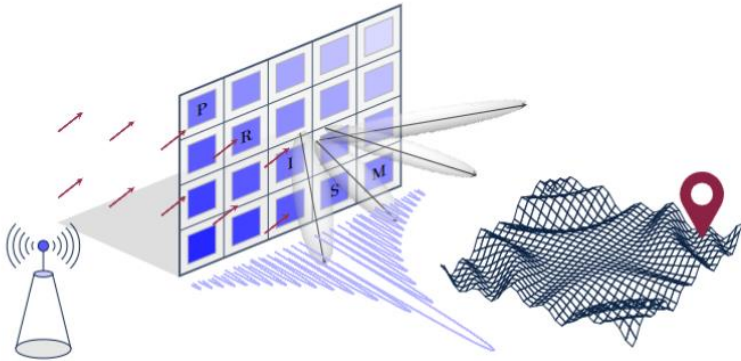


## NAVISP EL1-063: RIS-AIDED WIRELESS LOCALIZATION AND MAPPING

*Final Presentation*



# Table of Contents



- **Introduction**
  - UPAT, Prof. Vassilis Paliouras, Coordinator
- **RIS Technology**
  - NKUA, Prof. George Alexandropoulos
- **PRISM Testbed Overview**
  - Loctio, Thodoris Spanos
- **PRISM Methodology and Outcome**
  - UPAT, Dimitris Kompostiotis
- **Conclusions**
  - UPAT, Prof. Vassilis Paliouras

# **PRISM Objective: RIS Potential for Localization and Mapping**

- Operation in FR1
- Performance in real-world setups
- Performance using 5G signals
- Feasibility of testbeds using COTS
- Implementation of algorithms exploiting RIS-aided ranging and angle measurements

# Overview of the RIS Technology

**Prof. George C. Alexandropoulos**

PRISM's Final Presentation

September 30, 2025



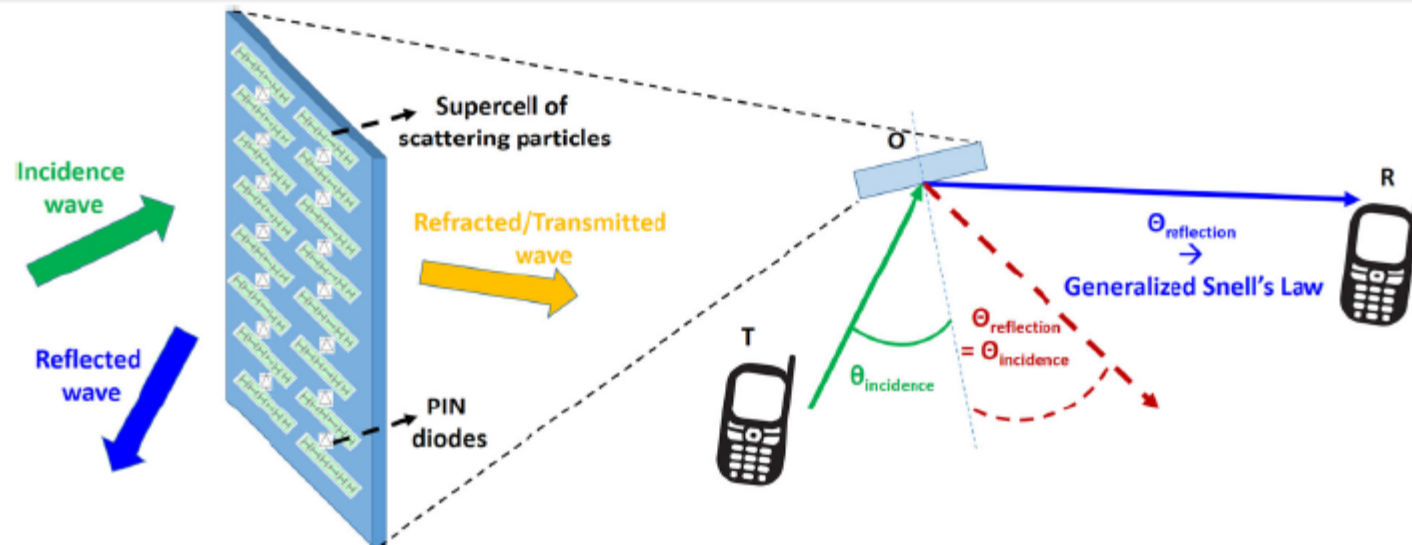
**National  
and Kapodistrian  
University of Athens**

Established in 1827



**Department of  
Informatics and Telecommunications**

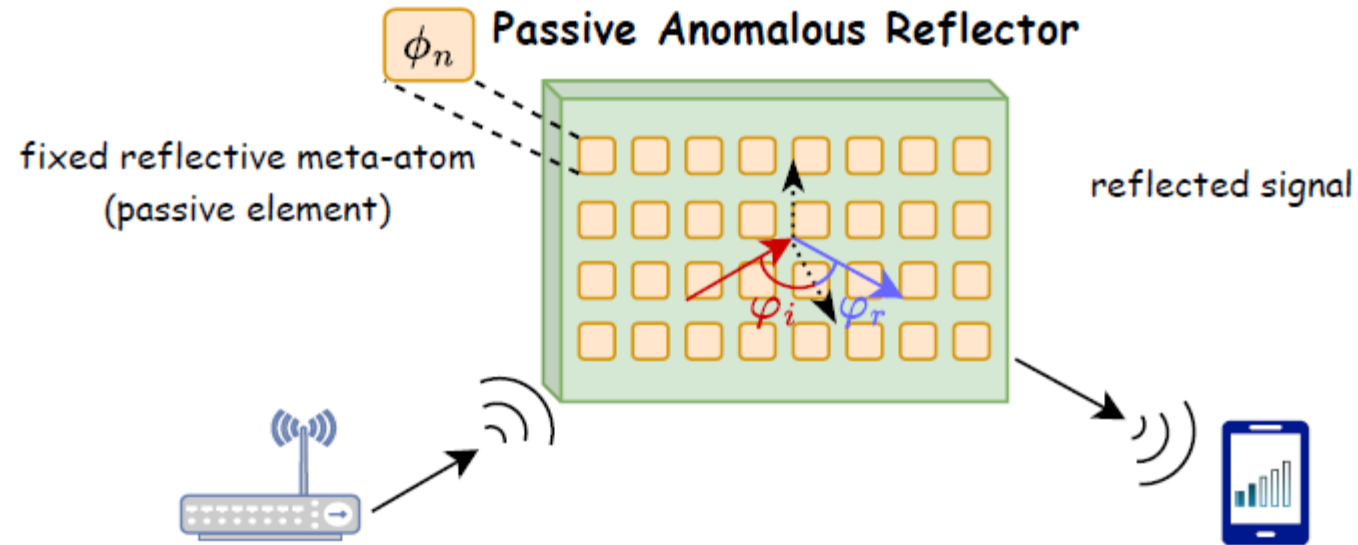
# Reconfigurable Intelligent Surfaces (RISs)



- RISs are being studied from a few GHz to subTHz.
- They operate at the basic level of propagation waves being capable of tuning the impinging electromagnetic field in the RF domain.
- They require a control unit for the dynamic control of their response to impinging waves.

M. Di Renzo, M. Debbah, D.-T. Phan-Huy, A. Zappone, M.-S. Alouini, C. Yuen, V. Sciancalepore, G. C. Alexandropoulos *et al.*, "Smart radio environments empowered by AI reconfigurable meta-surfaces: An idea whose time has come," *EURASIP JWCN*, May 2019. (EURASIP Best Paper Award 2021)

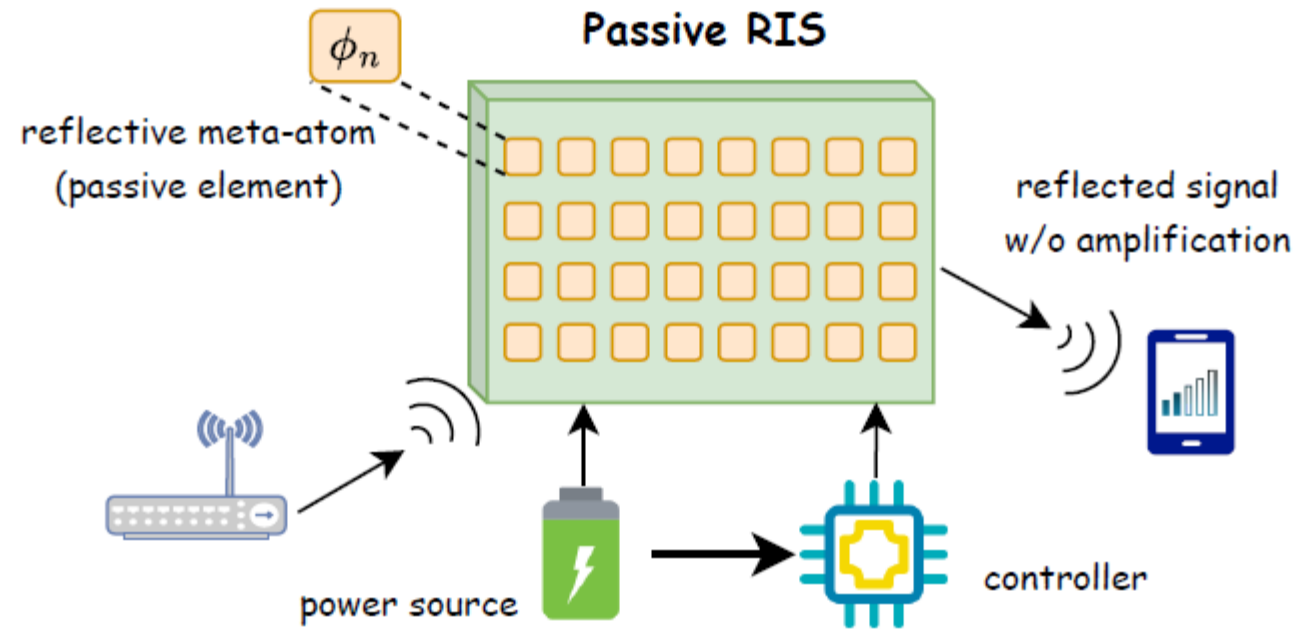
# Non-Reconfigurable Intelligent Surfaces



- Fixed anomalous reflection to enable virtual LOS paths.
- Phase configuration printed in hardware; reflection optimized for a fixed incoming signal angle.

E. Basar, G. C. Alexandropoulos, Y. Liu, Q. Wu, S. Jin, C. Yuen, O. Dobre, and R. Schober, "Reconfigurable intelligent surfaces for 6G: Emerging hardware architectures, applications, and open challenges," *IEEE VTM*, 2023.

# The Typical Passive (Almost) RIS



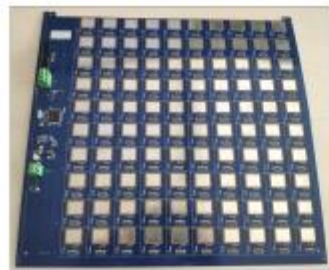
- The RIS controller needs power to maintain a phase profile and sweep among different ones. It usually serves as the interface between the RIS panel and the entity that wants to use it (e.g., the network).

E. Basar, G. C. Alexandropoulos, Y. Liu, Q. Wu, S. Jin, C. Yuen, O. Dobre, and R. Schober, "Reconfigurable intelligent surfaces for 6G: Emerging hardware architectures, applications, and open challenges," *IEEE VTM*, 2023.

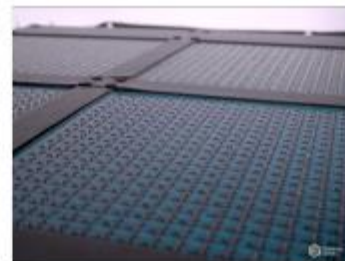
# RIS Prototypes in Different Frequency Bands



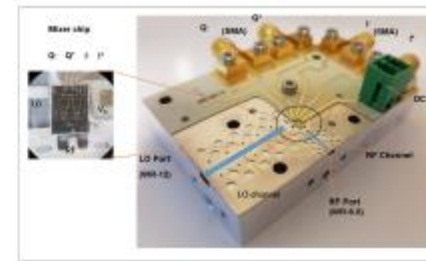
Varactor - 5.2GHz



RF-Switch - 5.3GHz



Pin diode - 27.31GHz

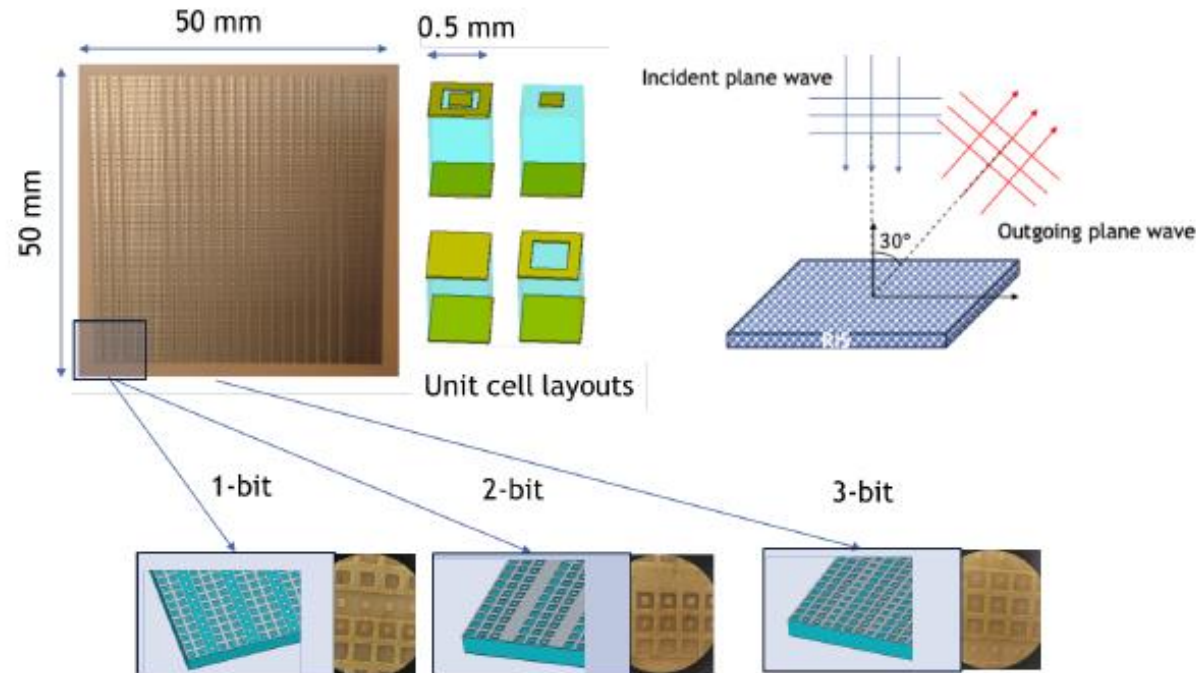


BiCMOS - 145GHz

RISE-6G public deliverables; available [here](#).



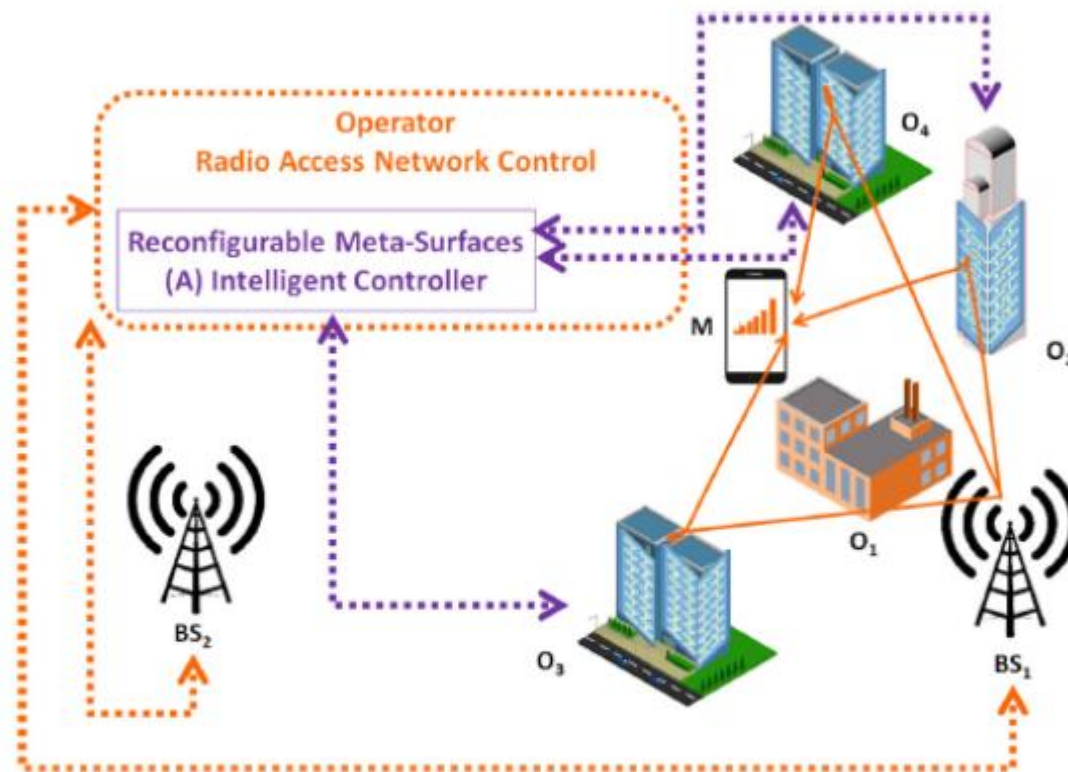
# RIS Prototype @304GHz and Channel Characterization



G. C. Alexandropoulos, A. Clemente, S. Matos, R. Husbands, S. Ahearne, Q. Luo, V. Lain-Rubio, T. Kürner, and L. M. Pessoa, "Reconfigurable intelligent surfaces for THz: Signal processing and hardware design challenges," *Proc. EUCAP*, 2024.

G. C. Alexandropoulos, L. H. W. Loeser, P. Gavrilidis, S. Matos, B. K. Jung, V. Elesina, A. Clemente, R. D'Errico, L. M. Pessoa, and T. Kürner, "Characterization of indoor RIS-assisted channels at 304 GHz: Experimental measurements, challenges, and future directions," *IEEE VTM*, 2025.

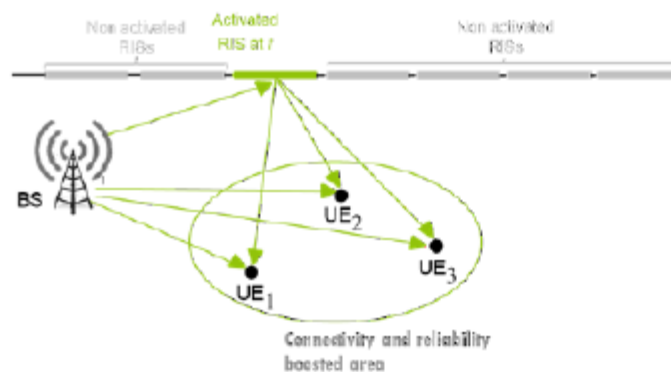
# Programmable Over-The-Air Signal Propagation



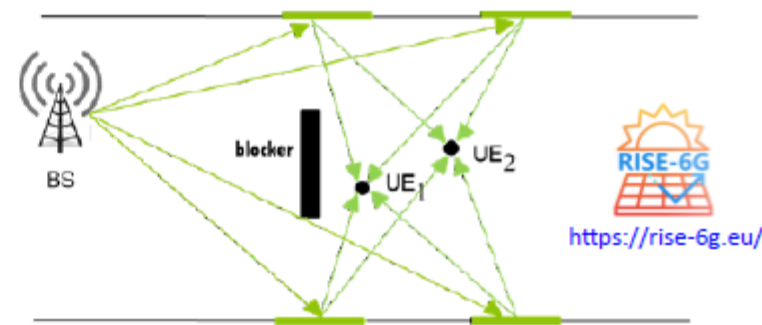
M. Di Renzo, M. Debbah, D.-T. Phan-Huy, A. Zappone, M.-S. Alouini, C. Yuen, V. Sciancalepore, G. C. Alexandropoulos *et al.*, "Smart radio environments empowered by AI reconfigurable meta-surfaces: An idea whose time has come," *EURASIP JWCN*, May 2019. (EURASIP Best Paper Award 2021)

C. Liaskos *et al.*, "A new wireless communication paradigm through software-controlled metasurfaces," *IEEE COMMAG*, 2018.

# RIS Deployment Scenarios

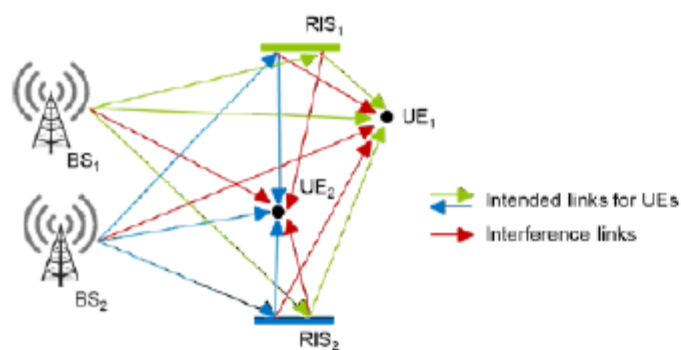


(a) Connectivity and reliability boosted by a single RIS.

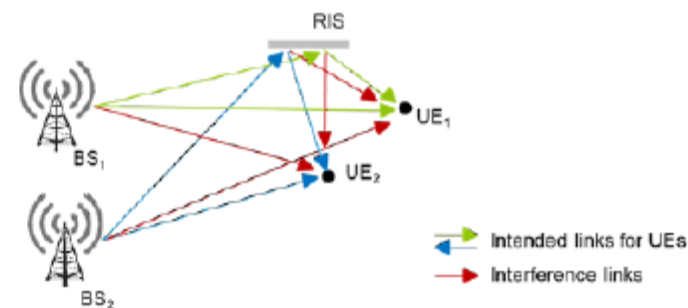


Connectivity and reliability enabled by multiple RIS

(a) RIS-aided systems where connectivity is enabled by multiple RISs.



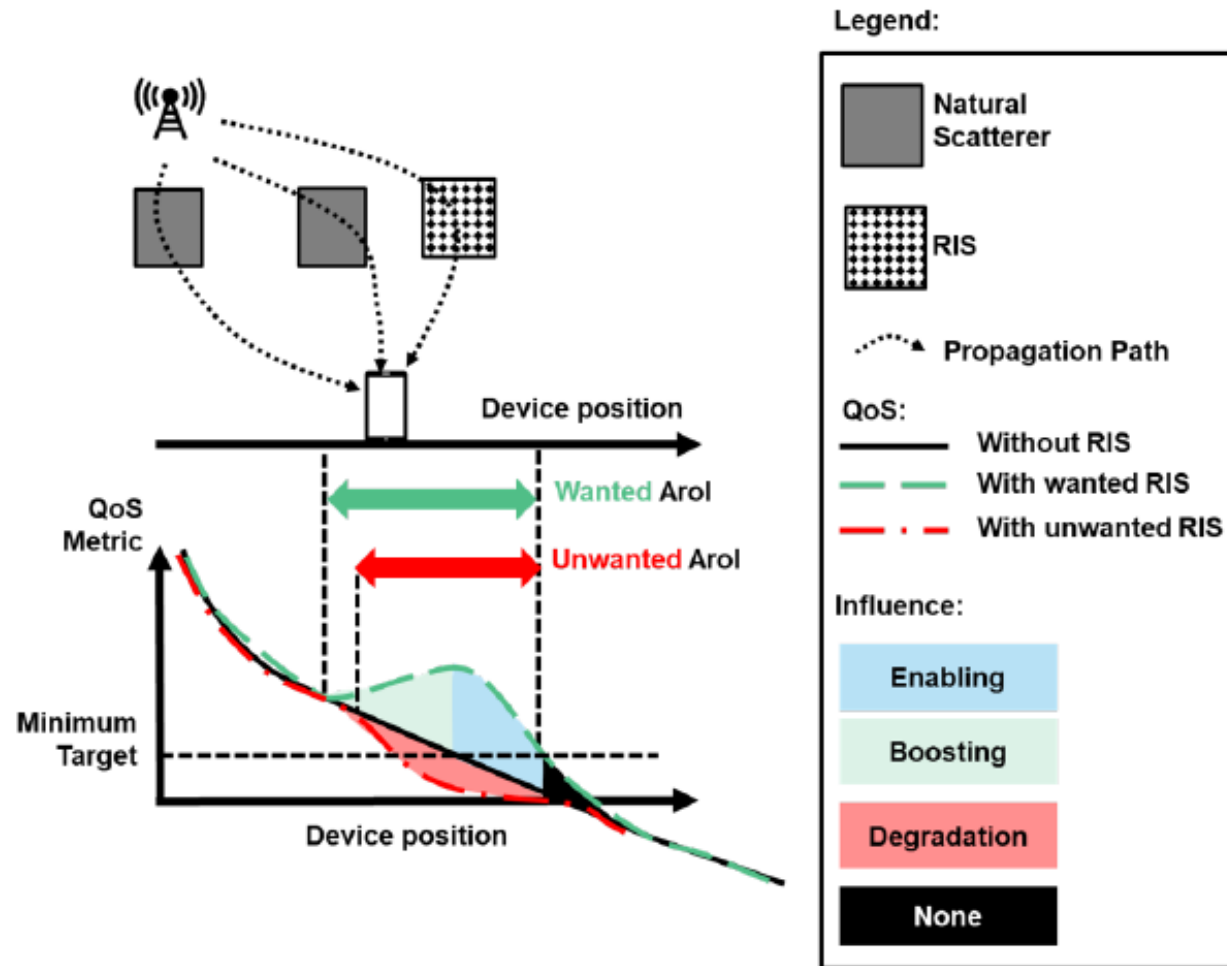
(b) RIS-empowered downlink communication of two BS-UE pairs, where each RIS can be controlled individually by each pair.



(b) A multi-tenancy scenario with two BS-UE pairs and a shared RIS that is optimized to simultaneously boost reliable communications.

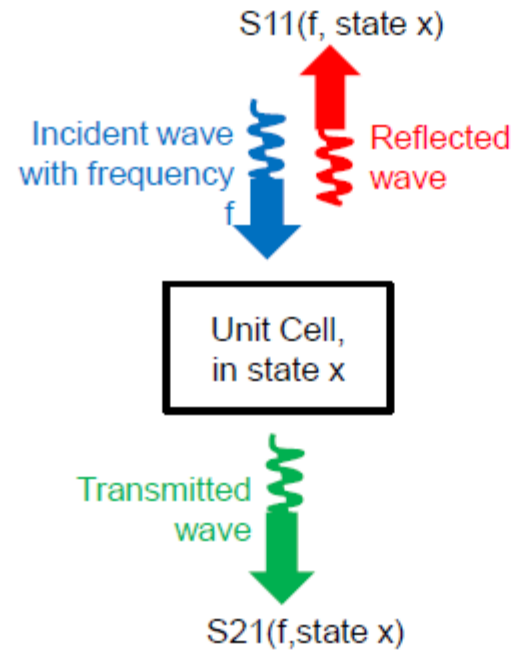
G. C. Alexandropoulos *et al.*, "RIS-enabled smart wireless environments: Deployment scenarios, network architecture, bandwidth and area of influence," *EURASIP JWCN*, 2023.

# The RIS Area of Influence



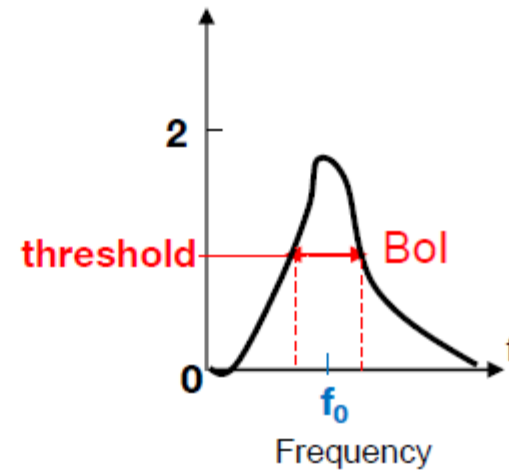
G. C. Alexandropoulos *et al.*, "RIS-enabled smart wireless environments: Deployment scenarios, network architecture, bandwidth and area of influence," *EURASIP JWCN*, 2023.

# The RIS Bandwidth of Influence



a) S-Parameters for state  $x$

Maximum Contrast in S-Parameters between states

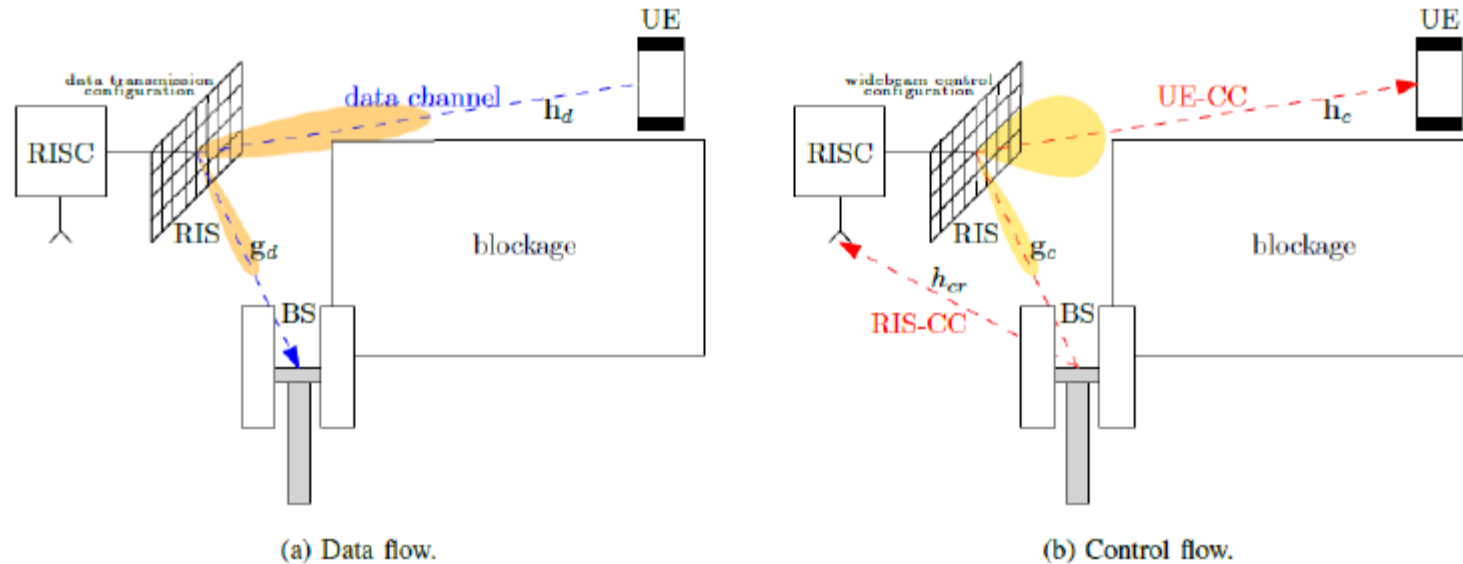


b)  $f_0$  and  $Bol$  definitions

G. C. Alexandropoulos *et al.*, "RIS-enabled smart wireless environments: Deployment scenarios, network architecture, bandwidth and area of influence," *EURASIP JWCN*, 2023.



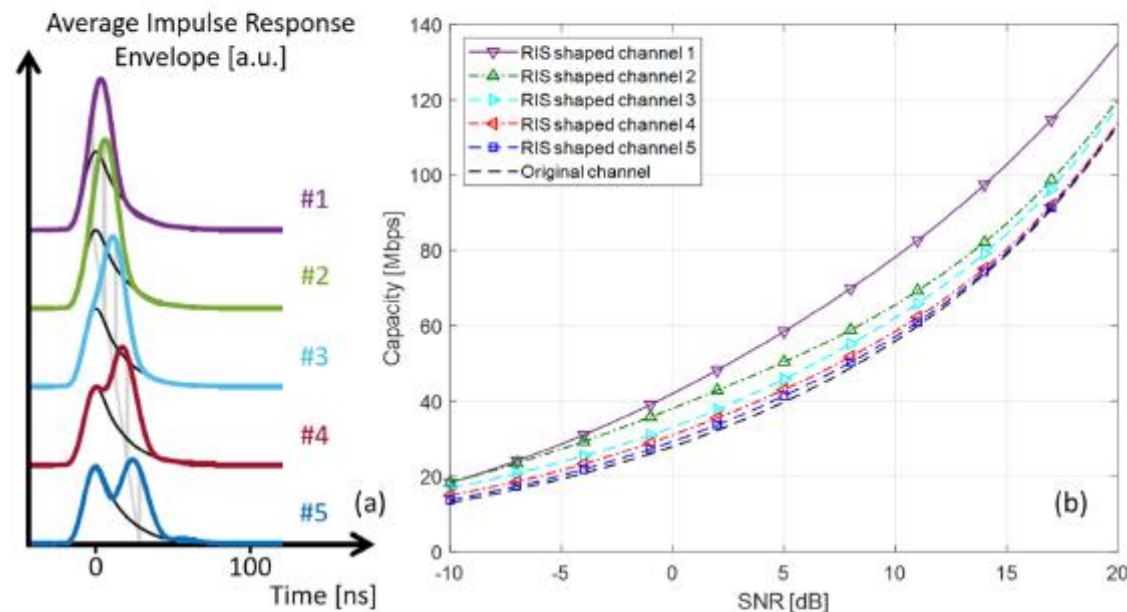
# Efficient Control Channels for RISs



- 4 phases: setup, algorithmic, acknowledgement, and payload.
- 2 generic schemes for the algorithmic phase: explicit channel estimation, codebook-based beam sweeping.
- Control channels: in-band, out-of-band.

F. Saggese, V. Croisfelt, R. Kotaba, K. Stylianopoulos, G. C. Alexandropoulos, and Petar Popovski, "On the impact of control signaling in RIS-empowered wireless communications," *IEEE OJCOM*, 2024.

# RIS-Enabled Over-the-Air Computing



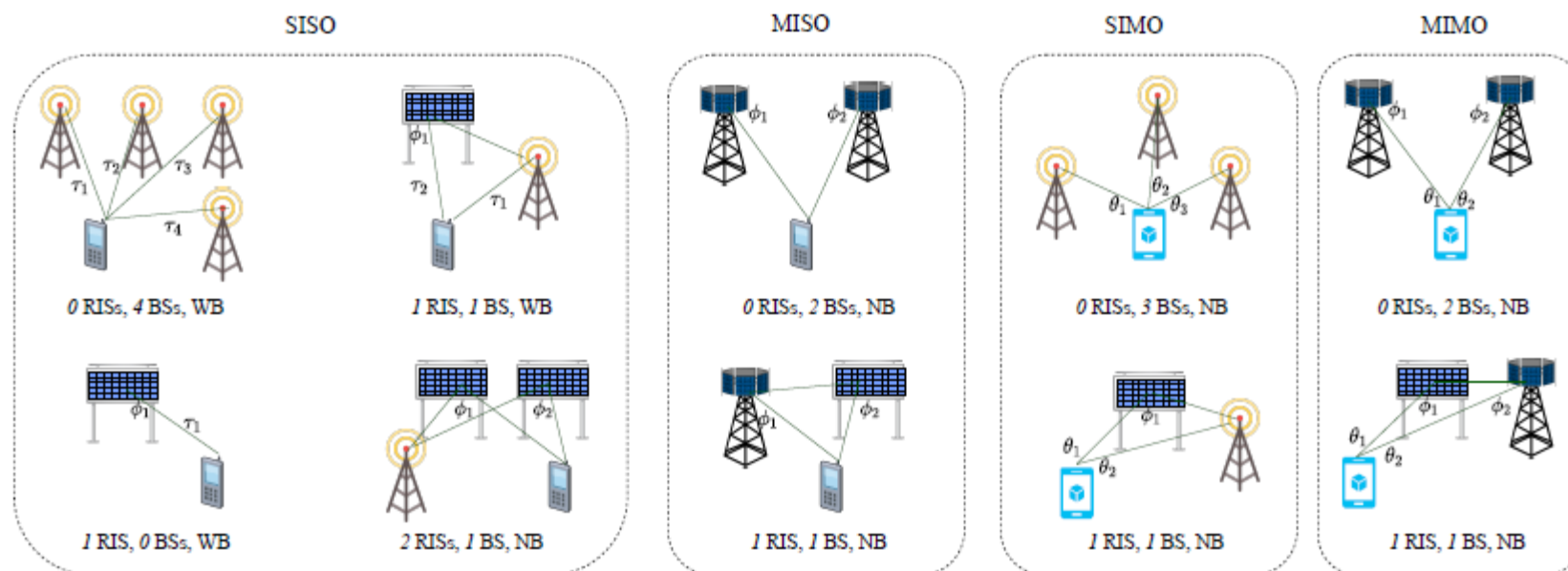
- RISs enable wave propagation control, even in rich scattering environments, acting as analog processors, as opposed to using traditional electronic processors at the communication ends.

---

G. C. Alexandropoulos, N. Shlezinger, and P. del Hougne, "Reconfigurable intelligent surfaces for rich scattering wireless communications: Recent experiments, challenges, and opportunities," *IEEE COMMAG*, 2021.

C. Huang, S. Hu, G. C. Alexandropoulos, A. Zappone, C. Yuen, R. Zhang, M. Di Renzo, and M. Debbah, "Holographic MIMO surfaces for 6G wireless networks: Opportunities, challenges, and trends," *IEEE JSAC*, 2021. (IEEE ComSoc F. W. Ellersick Prize 2023)

# Enabling 3D Localization with Purely Reflective RISs

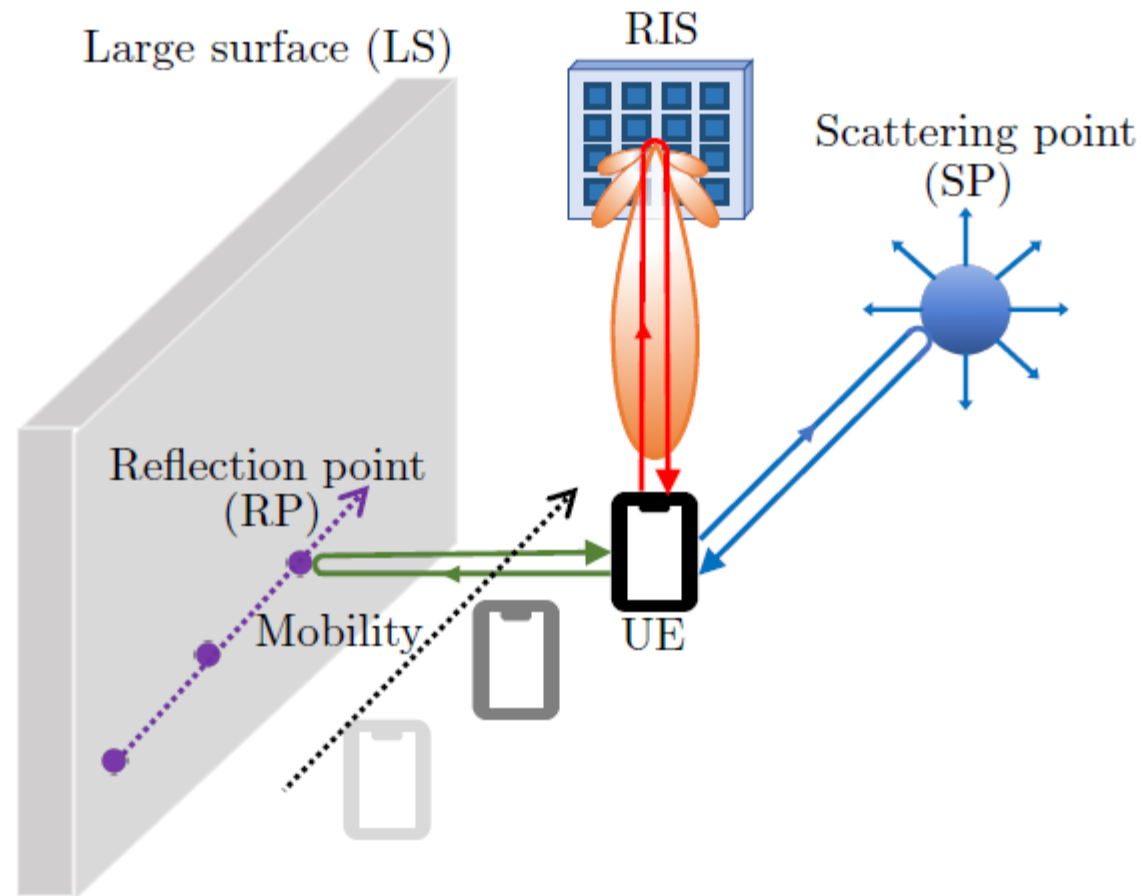


K. Keykhosravi, B. Denis, G. C. Alexandropoulos, Z. S. He, A. Albanese, V. Sciancalepore, and H. Wymeersch, "Leveraging RIS-enabled smart signal propagation for solving infeasible localization problems," *IEEE VTM*, 2023.

H. Chen, H. Kim, M. Ammous, G. Seco-Granados, G. C. Alexandropoulos, S. Valaee, and H. Wymeersch, "RISs and sidelink communications in smart cities: The key to seamless localization and sensing," *IEEE COMMAG*, 2023.

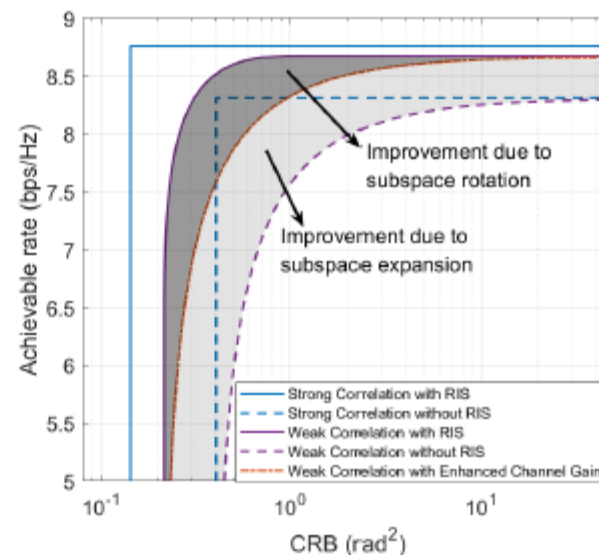
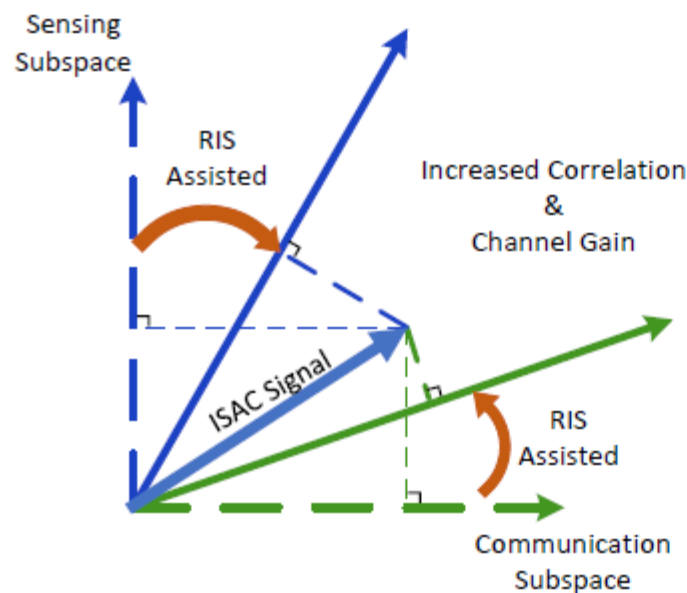


# RIS-Enabled and Access-Point-Free SLAM



H. Kim, H. Chen, M. F. Keskin, Y. Ge, K. Keykhosravi, G. C. Alexandropoulos, S. Kim, and H. Wymeersch, "RIS-enabled and access-point-free simultaneous radio localization and mapping," *IEEE TWC*, 2024.

# Programmable Subspace Correlation



- An RIS provides additional channel paths, and consequently channel gains, for both sensing and communications, which is equivalent to expanding the respective subspaces.
- Via RIS optimization, nearly orthogonal sensing and communications subspaces can be rotated to become coupled/correlated between each other; this is the regime where ISAC provides substantial gains.
- Hence, RISs can significantly improve the ISAC trade-off performance.

S. P. Chepuri, N. Shlezinger, F. Liu, G. C. Alexandropoulos, S. Buzzi, and Y. C. Eldar, "Integrated sensing and communications with reconfigurable intelligent surfaces," *IEEE SPM*, 2023.

# Network-Controlled Repeaters in 3GPP Release 18

## **RAN1** led - Radio Layer 1 (Physical layer)

- MIMO Evolution for Downlink and Uplink
- Study on Artificial Intelligence (AI)/Machine Learning (ML) for NR Air Interface
- Study on Evolution of NR Duplex Operation
- NR sidelink evolution
- Study on expanded and improved NR positioning
- Further NR RedCap UE complexity/cost reduction
- Study on network energy savings
- Further NR coverage enhancements
- NR Network-Controlled Repeaters**
- Enh. of NR Dynamic spectrum sharing (DSS)
- Study on low-power Wake-up Signal and Receiver for NR
- Multi-carrier enhancements for NR

# The ETSI ISG RIS

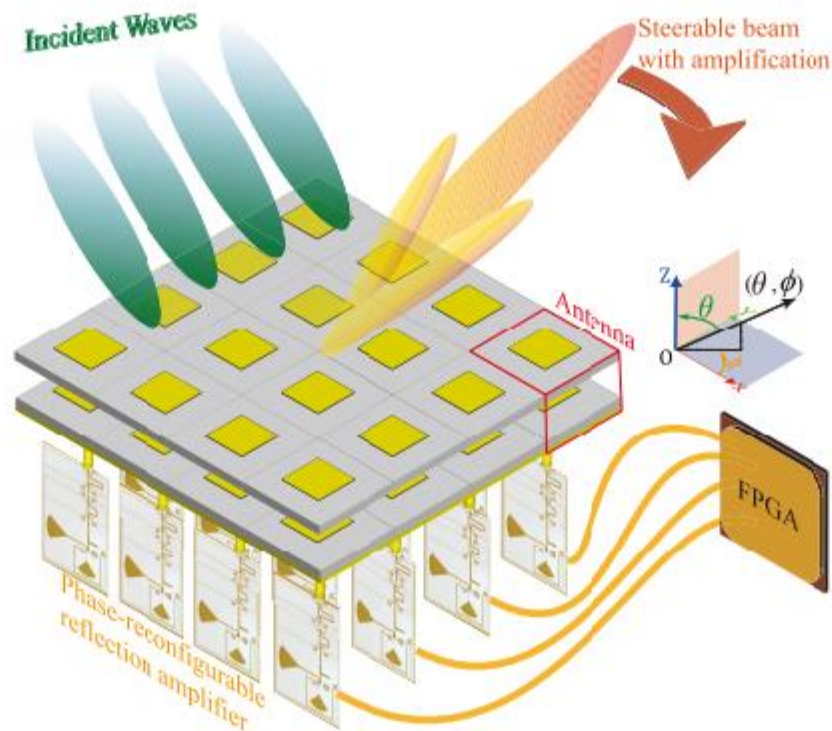
Identifier	Title	Main objectives	Estimated publication time
DGR RIS 004	Implementation and practical considerations	Investigation of implementation and practical considerations for RISs in a wide range of frequency bands and deployment scenarios; consult possible solutions and prototyping results.	August 2024
DGR RIS 005	Diversity and multiplexing of RIS-aided communications	Identification of use cases and deployment scenarios of RIS-based diversity and multiplexing schemes. Investigation of feasible diversity and multiplexing schemes for different RIS hardware and operating modes, while identifying the TX/RX complexity increase or reduction for the various multiplexing schemes. Evaluate the characteristics of RIS-aided channels for different diversity schemes and analyze the performance gains and impact.	July 2024
DGR RIS 006	Multi-functional reconfigurable intelligent surfaces (RIS): Modeling, Optimization, and operation	Identification of challenges and inclusion of efficient solutions for multi-functional RISs (MF-RISs). Channel modeling, phase profile optimization, resource allocation, and practical deployment schemes for MF-RISs.	September 2024
DGR RIS 007	Near-field channel modeling and mechanics	a) Identification of use cases and scenarios for near-field RIS-aided wireless systems; b) channel modeling for RIS-aided communications in the near-field region, also including methods to characterize the cascaded TX-RIS-RX channel; c) Investigation of technical solutions/mechanisms applicable for RIS-assisted wireless systems in the near field; and d) identification and analysis of potential specification impact to standards.	December 2025

---

R. Liu, S. Zheng, Y. Jiang, Q. Wu, N. Zhang, Y. Liu, M. Di Renzo, and G. C. Alexandropoulos, "Sustainable wireless networks via reconfigurable intelligent surfaces (RISs): Overview of the ETSI ISG RIS," *IEEE COMSTD*, 2025.



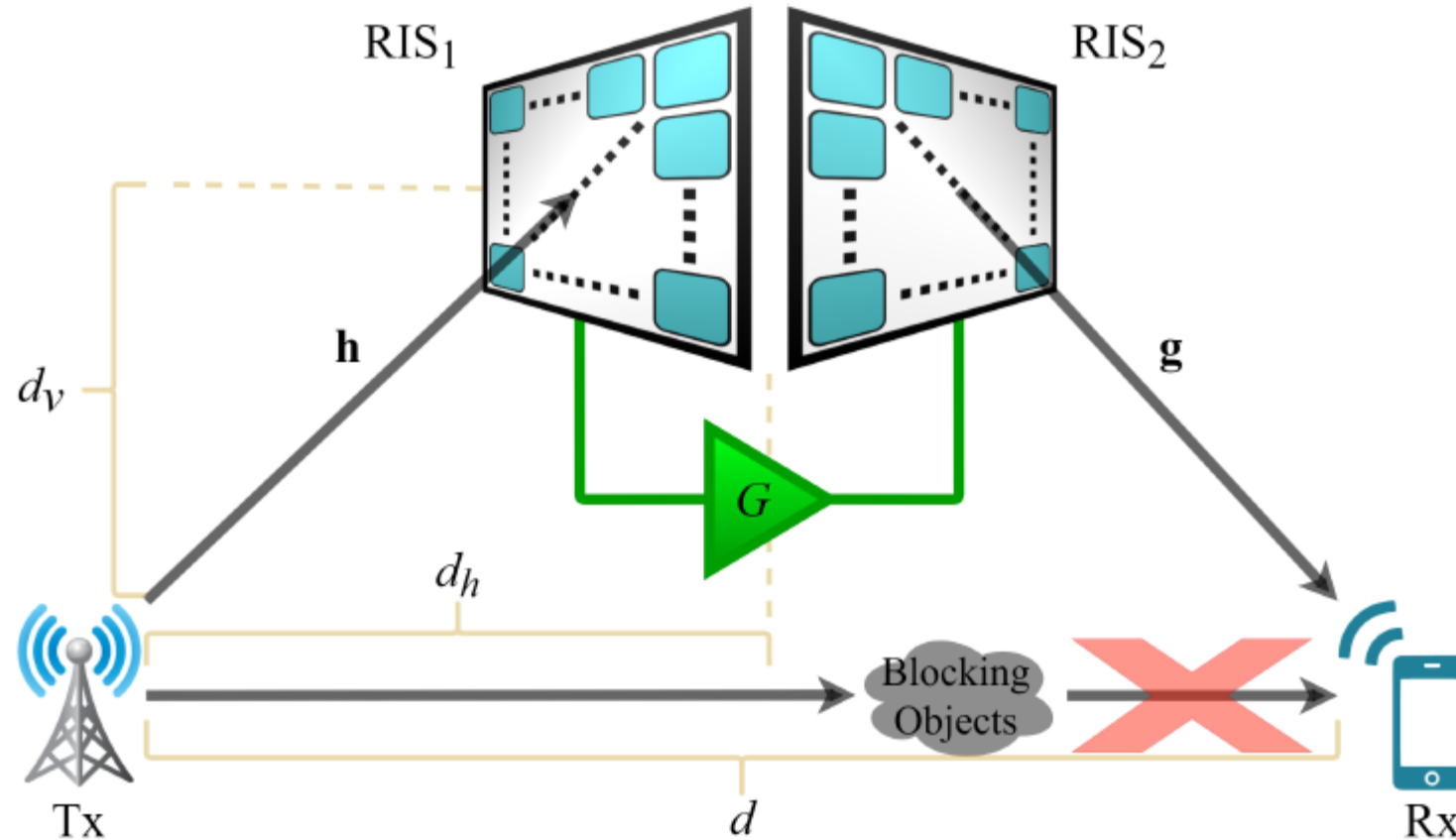
# RISs with Reflection Amplification Elements



J. Rao, Y. Zhang, S. Tang, Z. Li, C. -Y. Chiu, and R. Murch, "An active reconfigurable intelligent surface utilizing phase-reconfigurable reflection amplifiers," *IEEE TMTT*, 2023.

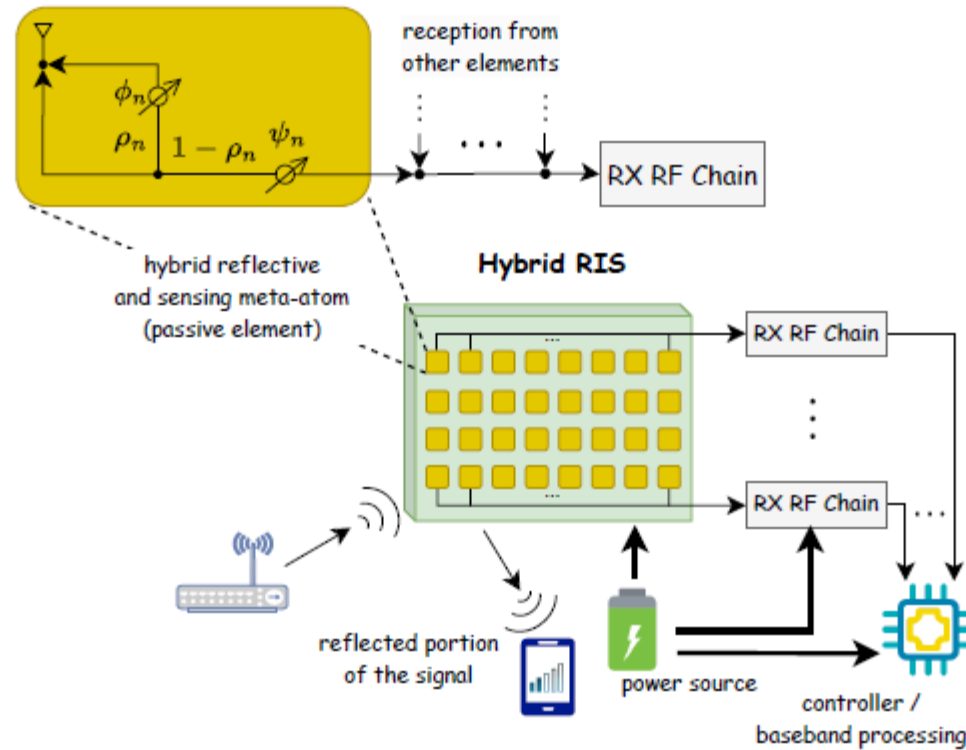
P. Gavrilidis, D. Mishra, B. Smida, E. Basar, C. Yuen, and G. C. Alexandropoulos, "Active reconfigurable intelligent surfaces: Circuit modeling and reflection amplification optimization," *IEEE OJCOM*, 2025.

# RISs with an Embedded Amplifier



R. Akif Tasci, F. Kilinc, E. Basar, and G. C. Alexandropoulos, "A new RIS architecture with a single power amplifier: Energy efficiency and error performance analysis," *IEEE Access*, 2022.

# Simultaneous Reflecting and Sensing RISs

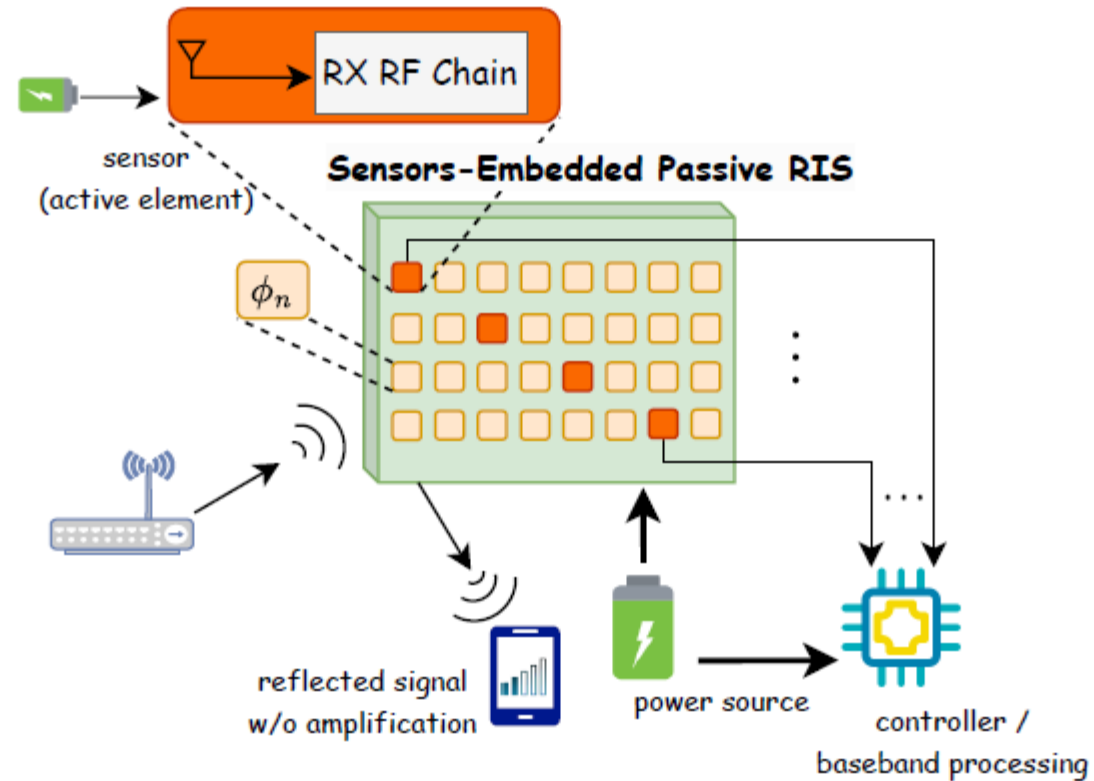


G. C. Alexandropoulos and E. Vlachos, "A hardware architecture for reconfigurable intelligent surfaces with minimal active elements for explicit channel estimation," *IEEE ICASSP*, 2020.

I. Alamzadeh, G. C. Alexandropoulos, N. Shlezinger, and M. F. Imani, "A reconfigurable intelligent surface with integrated sensing capability," *Scientific Reports*, 2021.

G. C. Alexandropoulos, N. Shlezinger, I. Alamzadeh, M. F. Imani, H. Zhang, and Y. C. Eldar, "Hybrid reconfigurable intelligent metasurfaces: Enabling simultaneous tunable reflections and sensing for 6G wireless communications," *IEEE VTM*, 2023.

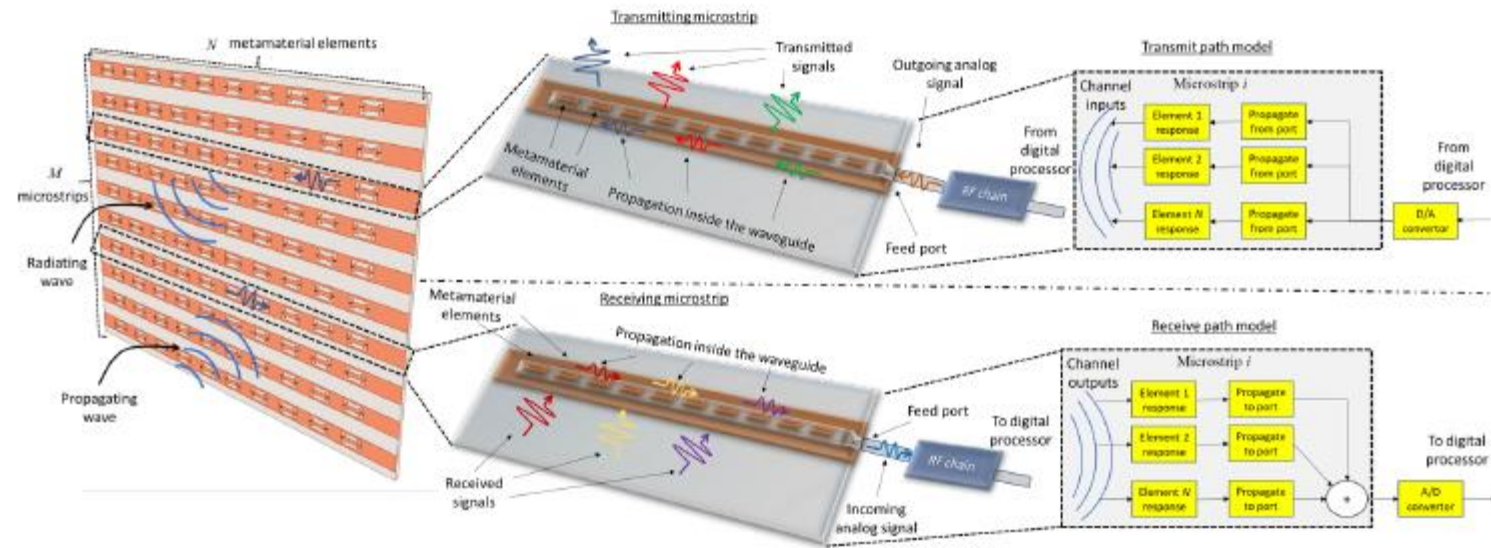
# RISs with Embedded Sensors



A. Taha, M. Alrabeiah, and A. Alkhateeb, "Enabling large intelligent surfaces with compressive sensing and deep learning," *IEEE Access*, 2021.



# Dynamic Metasurface Antennas



N. Shlezinger, G. C. Alexandropoulos, M. F. Imani, Y. C. Eldar, and D. R. Smith, "Dynamic metasurface antennas for 6G extreme massive MIMO communications," *IEEE WCOM*, 2021. (IEEE ComSoc Fred Ellersick Prize 2024)

E. Vlachos, G. C. Alexandropoulos, and J. Thompson, "Wideband MIMO channel estimation for hybrid beamforming millimeter wave systems via random spatial sampling," *IEEE JSTSP*, 2019.

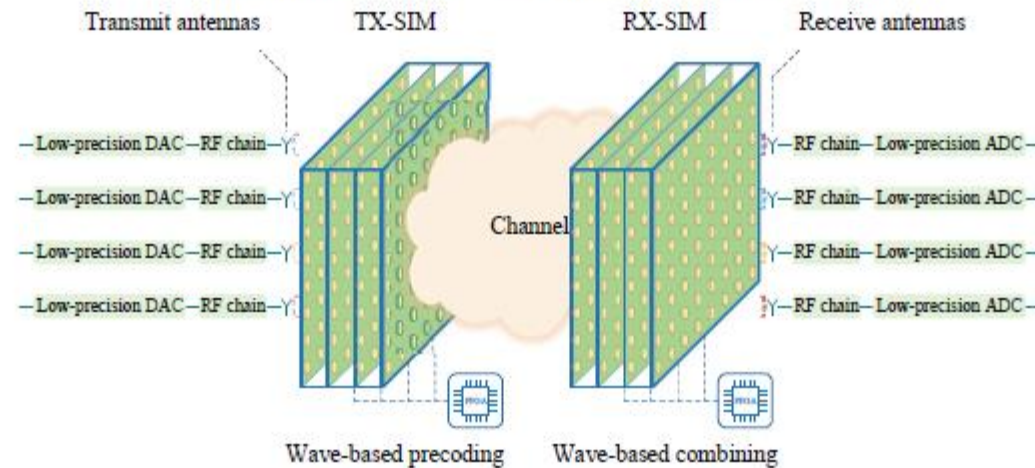
C. Huang, S. Hu, G. C. Alexandropoulos, A. Zappone, C. Yuen, R. Zhang, M. Di Renzo, and M. Debbah, "Holographic MIMO surfaces for 6G wireless networks: Opportunities, challenges, and trends," *IEEE WCOM*, 2020. (IEEE ComSoc Fred Ellersick Prize 2023)

T. Gong, P. Gavrilidis, R. Ji, C. Huang, G. C. Alexandropoulos, L. Wei, Z. Zhang, M. Debbah, H. V. Poor, and C. Yuen, "Holographic MIMO 6G communications: Theoretical foundations, enabling technologies, and future directions," *IEEE Commun. Surveys & Tuts.*, 2024.

# Stacked Intelligent Metasurfaces



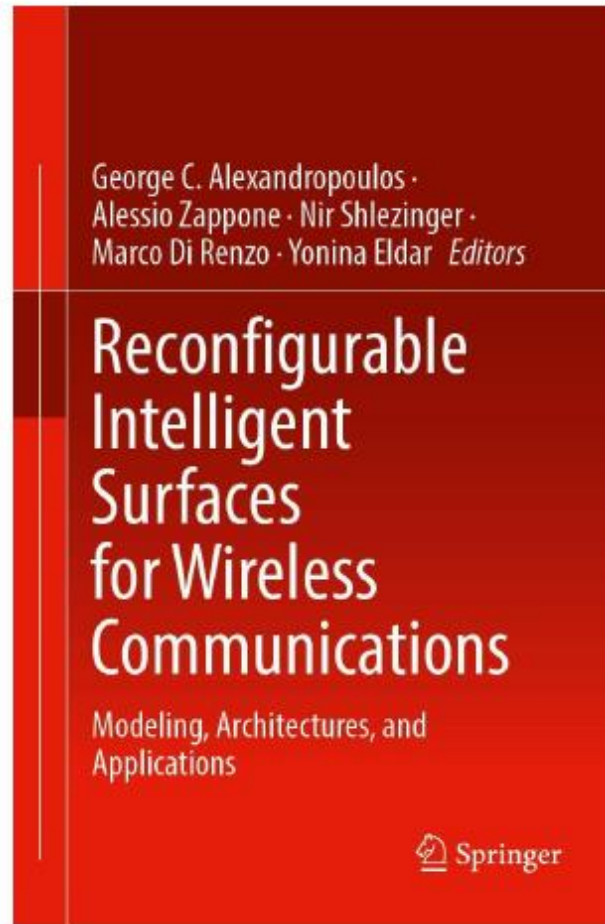
(a) Conventional MIMO transmission: Parallel subchannels in the eigenspace.



(b) SIM-aided HMIMO transmission: Parallel subchannels in the physical space.

J. An, C. Xu, D. W. K. Ng, G. C. Alexandropoulos, C. Huang, C. Yuen, and L. Hanzo, "Stacked intelligent metasurfaces enabling efficient holographic MIMO communications for 6G," *IEEE JSAC*, 2023.

# A Book on RISs for Wireless Communications



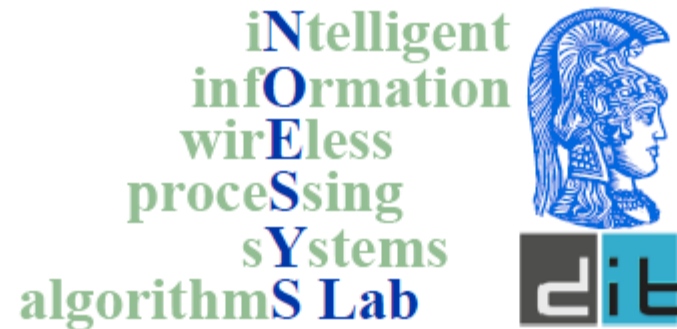
G. C. Alexandropoulos, A. Zappone, N. Shlezinger, M. Di Renzo, and Y. C. Eldar, *Reconfigurable Intelligent Surfaces for Wireless Communications: Modeling, Architectures, and Applications*, Springer Nature Singapore, 2025.

Thank you for your attention

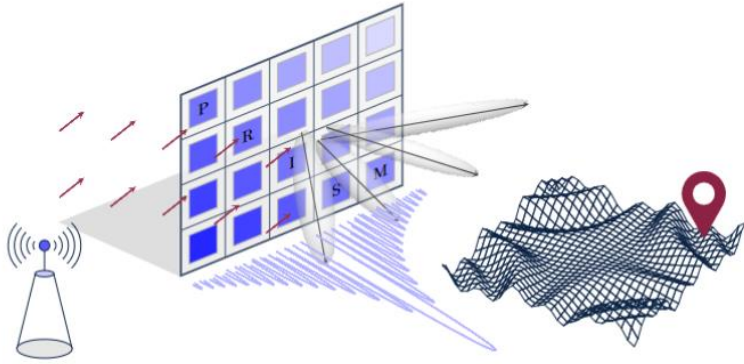
**Prof. George C. Alexandropoulos**

e-mail: [alexandg@di.uoa.gr](mailto:alexandg@di.uoa.gr)

URL: [www.alexandropoulos.info](http://www.alexandropoulos.info)







## PRISM Testbed Overview

- Introduction
- RIS Technology
  - NKUA, Prof. George Alexandropoulos
- **PRISM Testbed Overview**
  - Loctio, Thodoris Spanos
- PRISM Methodology and Outcome
  - UPAT, Dimitris Kompostiotis
- Conclusions
  - UPAT, Prof. Vassilis Paliouras

- Core COTS Components
- Calibration Procedures
- 5G PRS Signal as Test Waveform
- Test Environments

# Testbed components

- ❖ Reconfigurable Intelligent Surface
- ❖ USRP X300 (Tx side)
  - Wide instantaneous bandwidth to support 5G NR-compliant signals and high-resolution ranging
- ❖ USRP N310 (Rx side)
  - Multiple, phase-coherent channels in a single device, essential for Angle of Arrival (AoA) estimation algorithms
- ❖ LNAs (Rx side)
  - To improve receiver sensitivity
- ❖ Directive flat panel antennas (ITELITE)
  - Approx. 20° HPBW, suitable for focused transmission and reception
- ❖ Omni antennas
  - Single-element antenna
  - Three-element Uniform Linear Array
- ❖ Flexibility of testbed

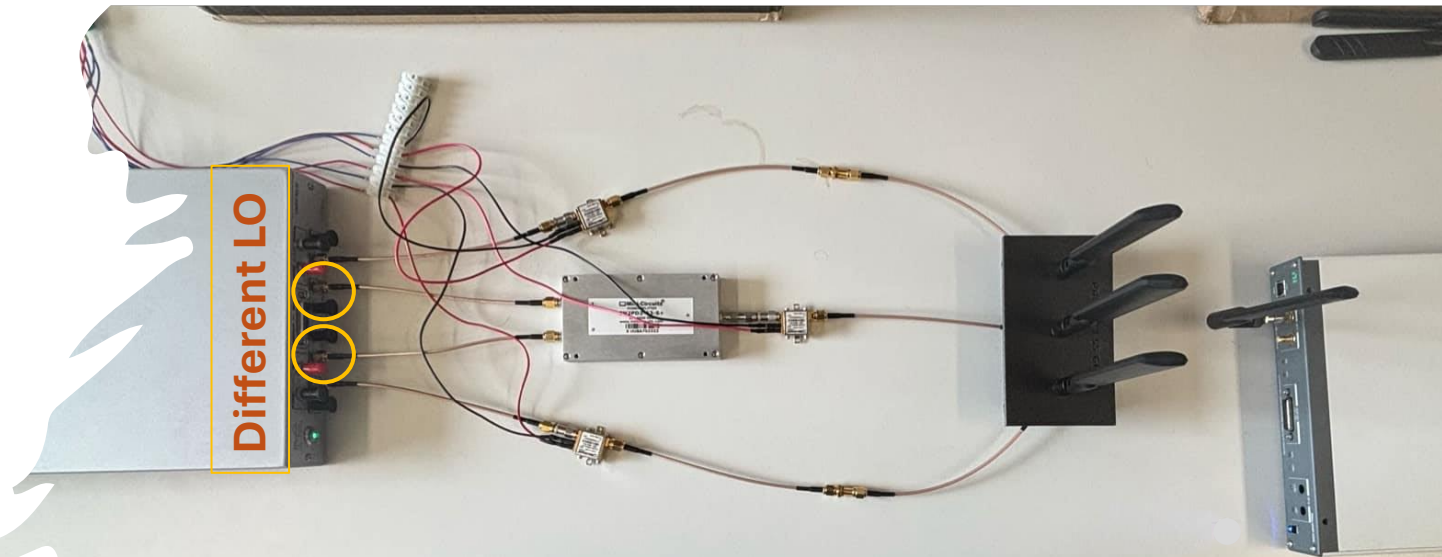
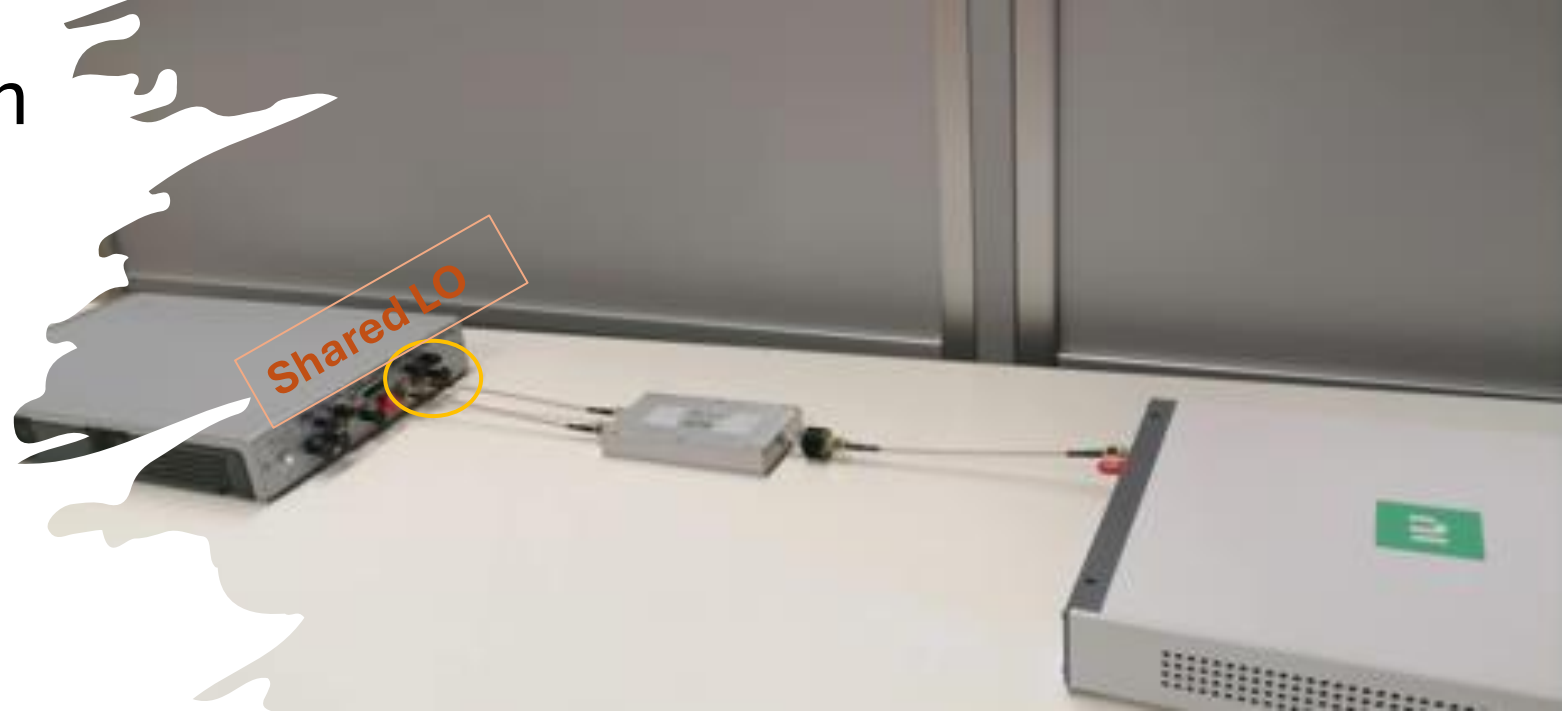


# Phase Offset and Calibration of USRP Channels

**Challenge:** Inherent phase mismatches between USRP RF channels, which degrade the accuracy of AoA algorithms such as MUSIC

## Two-Stage Calibration Strategy:

- A. Offline Calibration (**for channels with a shared LO**)
  - A common pilot signal is injected into the channels with the shared LO.
  - A static phase offset is measured and stored for a set of Tx/Rx gain values.
- B. Online Calibration (**for channels with different LOs**)
  - Independent LOs can drift over time, requiring real-time correction.
  - A 2-to-1 splitter is used to distribute a common reference signal to one channel of each LO group.





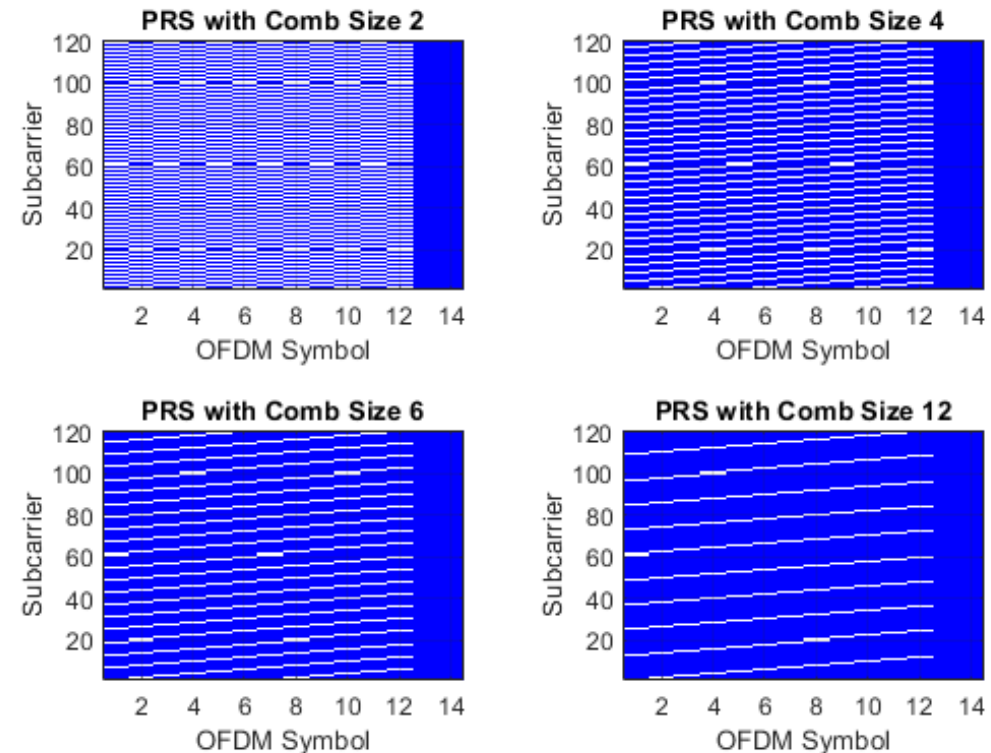
# 5G PRS Signal as Test Waveform

- Used for downlink positioning
- 31-bit Gold sequence
- Comb type structure
- Empty subcarriers that allow multi-transmission
- Different numerologies supporting a variety of SCS, and different BWs
- Up to 12 OFDM symbols per slot can contain PRS

## Selected PRS parameters:

- Numerology:  $\mu = 2$
- Subcarrier Spacing: 60 kHz
- Comb Size:  $K_{\text{Comb}}^{\text{PRS}} = 2$
- Bandwidth: 37.44 MHz
- Extended Cyclic Prefix  $\Rightarrow$  12 OFDM Symbols per slot

5G PRS Signals with Comb Patterns (14 OFDM Symbols per Slot)





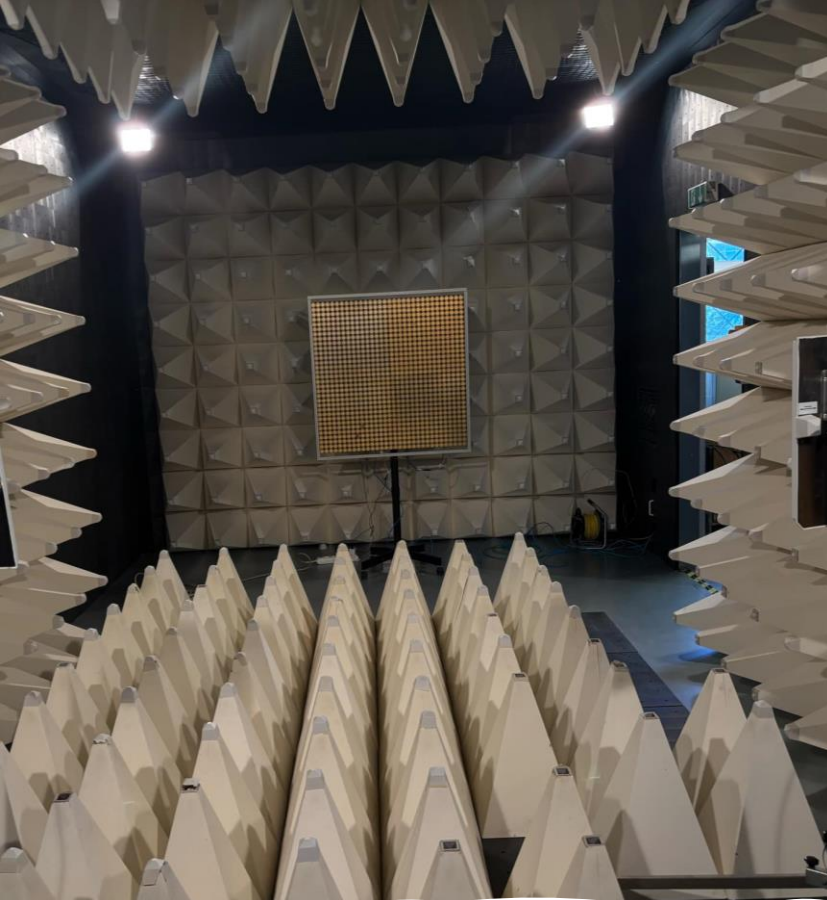


Photo: PRISM anechoic chamber setup at University of West Attica



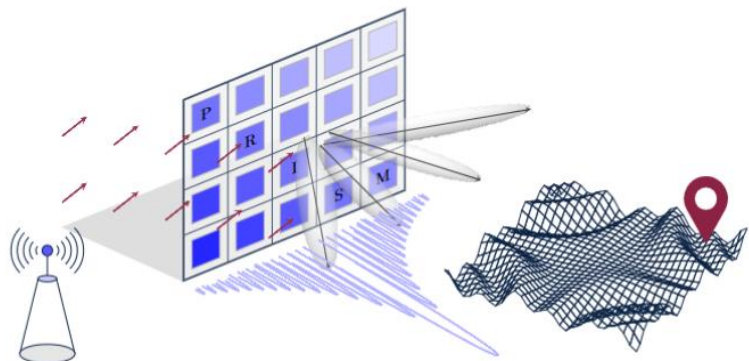
Photo: PRISM indoor setup at ECE Dept., UPAT



Photo: PRISM outdoor setup at VLSILAB, ECE Dept., UPAT

# Test Environments

- Anechoic chamber: reflection-free environment, limited space
- Outdoor environment: real-world conditions, low multipath
- Indoor environment: most challenging scenario, dense multipath

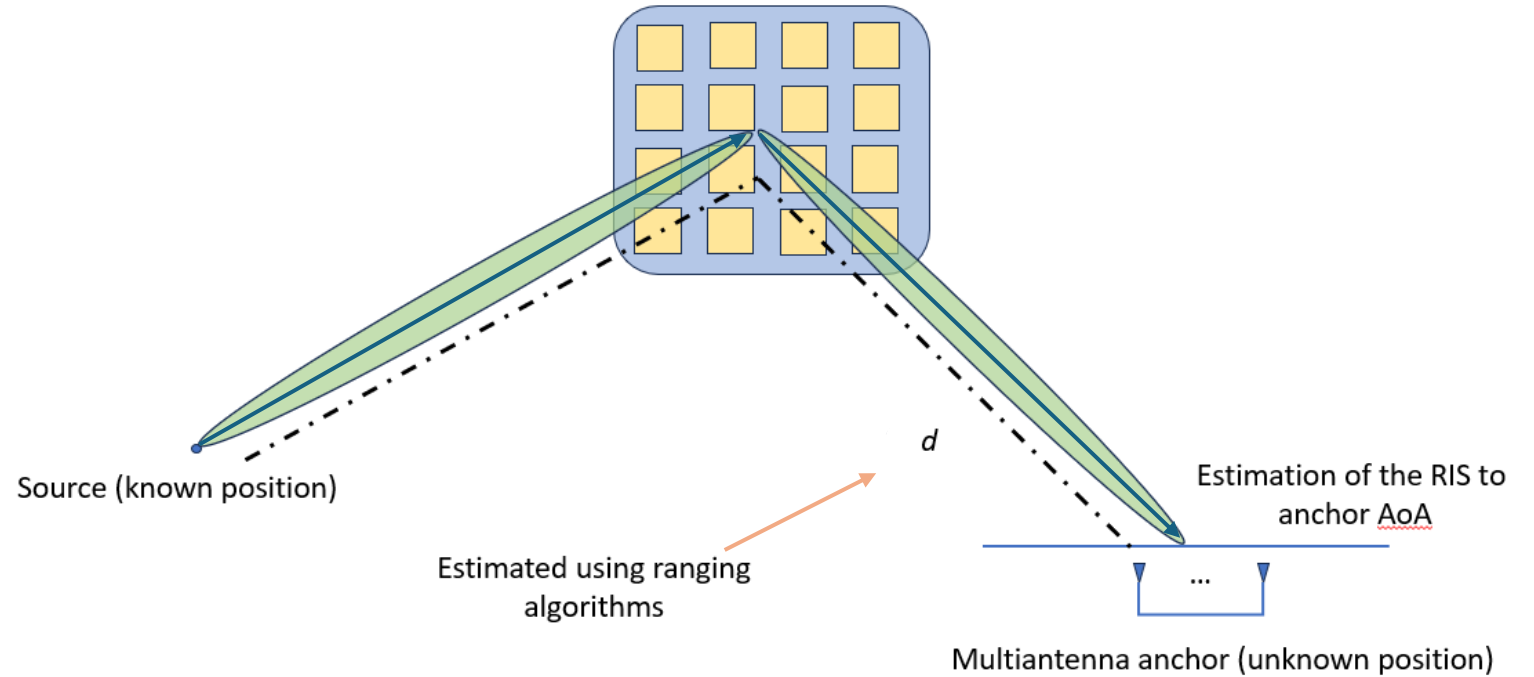


## PRISM Methodology and Outcome

- PRISM Motivational Scenario and Algorithmic Approach
- Core Contributions of the PRISM project
  - Beam Sweeping using RIS
  - RIS-Aided Angle of Arrival Estimation
  - RIS-Aided Ranging
  - RIS-Aided Mapping
- Conclusions

- Introduction
- RIS Technology
  - NKUA, Prof. George Alexandropoulos
- PRISM Testbed Overview
  - Loctio, Thodoris Spanos
- PRISM Methodology and Outcome
  - UPAT, Dimitris Kompostiotis
- Conclusions
  - UPAT, Prof. Vassilis Paliouras

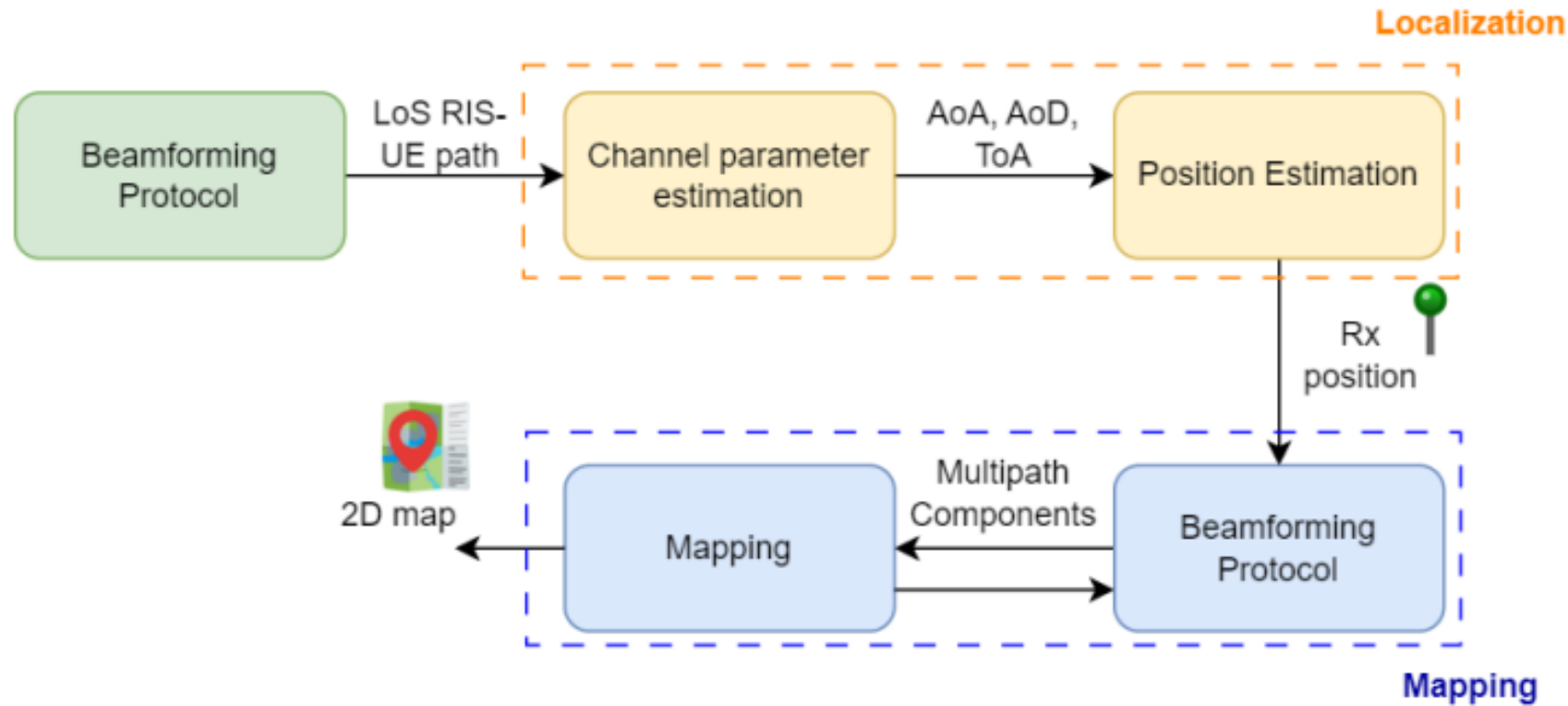
# RIS-Aided Positioning: A Motivational Scenario



- ✓ Uses the minimum possible number of anchor points
- ✓ Requires the implementation of both ranging and AoA/AoD estimation
- ✓ Does not require “common sense of time” reference in ToA estimation by exploiting the differential arrival of the direct and RIS-reflected paths

# Overview of the Algorithmic Approach for RIS-Aided Localization and Mapping

- **Localization**
  - Beam sweeping protocol (codebook-based RIS beamforming)
  - AoA estimation algorithms (e.g. MUSIC)
  - ToA estimation/Ranging algorithms
- **Mapping**
  - 1 scattering point is introduced in the considered setup
  - Prior knowledge of UE's position
  - Beamform towards the scattering point (codebook-based RIS beamforming)
  - Super resolution algorithms (e.g. MUSIC) or heatmap-based estimates are exploited for NLoS paths' detection.





# RIS Characterization

- ✓ Anechoic chamber, specular reflection
- ✓ Around the RIS working frequency, the theoretical phase shift is expected to be  $180^\circ$
- ✓ VNA Rohde & Schwarz ZVA24

## RIS prototype:

- RIS working frequency: 3.5 GHz
- $32 \times 32 = 1024$  elements
- 1-bit voltage control, varactor-based
- dual-polarized
- scanning range from  $-65$  to  $65$  degrees
- 10 ms configuration update time
- Raspberry Pi (RPI) controller for RIS configuration
  - Supports communication via TCP/IP over wireless or wired (Ethernet) connection

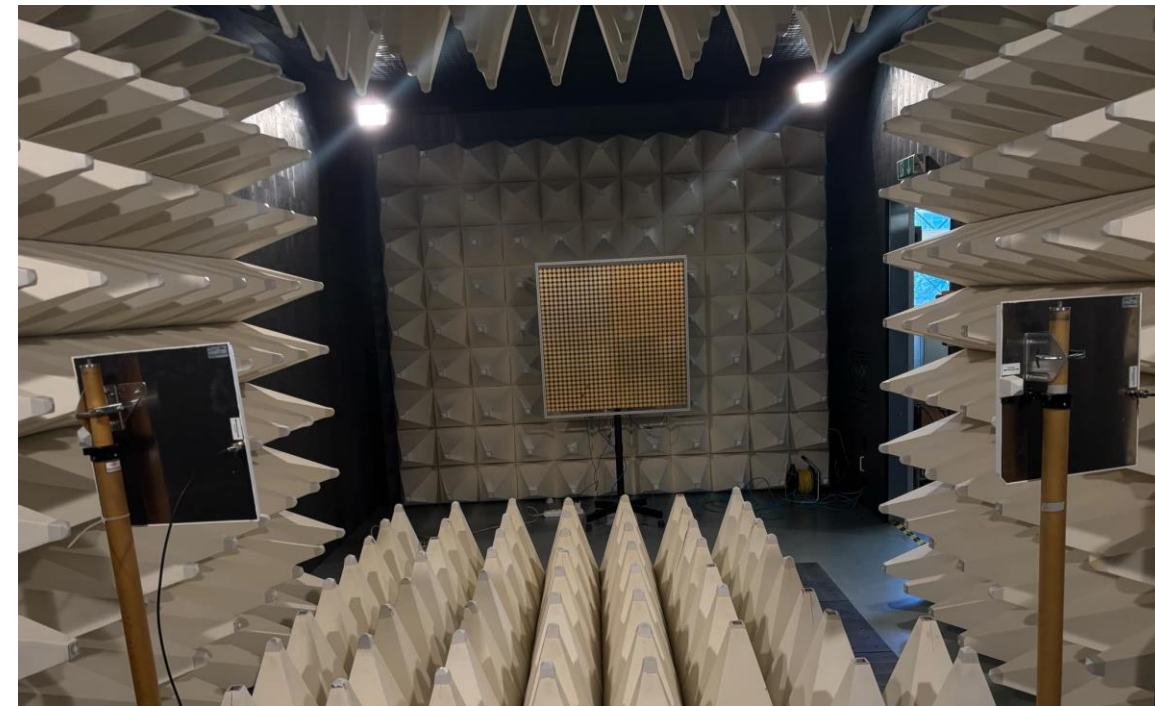
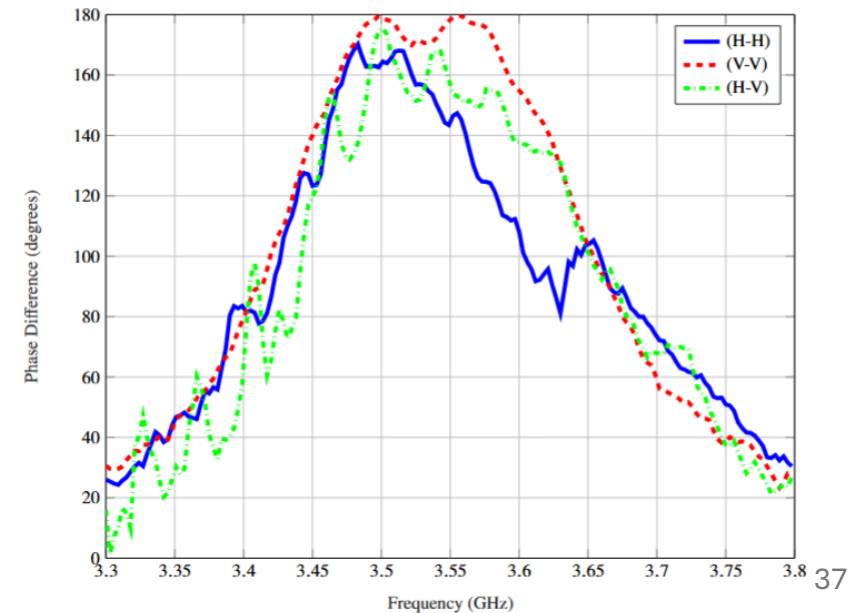
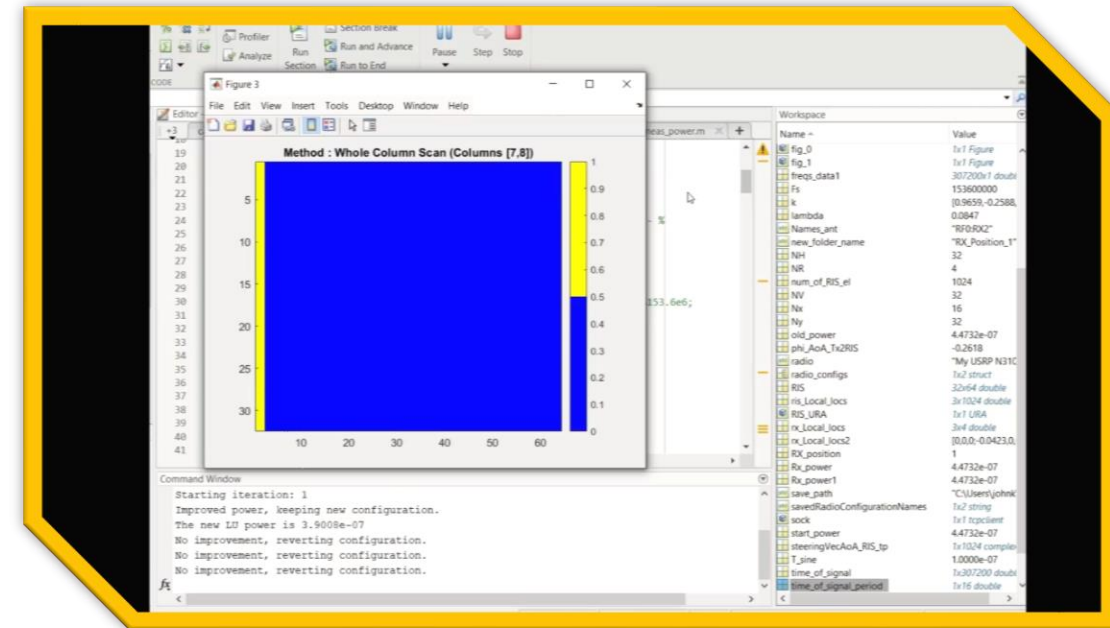


Photo: PRISM anechoic chamber setup at University of West Attica



# RIS Configuration Optimization for Beam Steering (Codebook Generation)

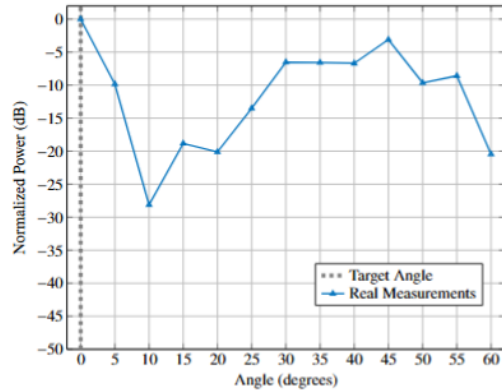
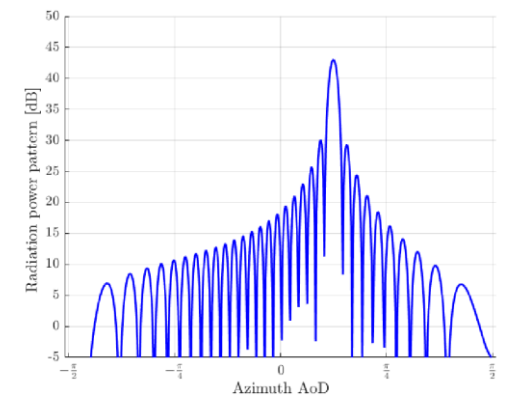
- **Objective:** Steer the main lobe of the RIS-reflected signal toward a desired Angle of Departure (AoD).
- **Challenge:** The lack of accurate models to capture the RIS radiation pattern prevents model-based beamforming design.
- **Approach:** A data-driven greedy algorithm is employed, where RIS phase configurations are iteratively adjusted and evaluated based on received power measurements.
- **Execution:** In each iteration, columns or rows of RIS elements are modified; if the change increases the received power, it is retained, otherwise it is discarded.
- **Advantage:** The algorithm adapts in real time to the propagation environment, enabling practical and efficient codebook generation without requiring prior calibration or channel models.



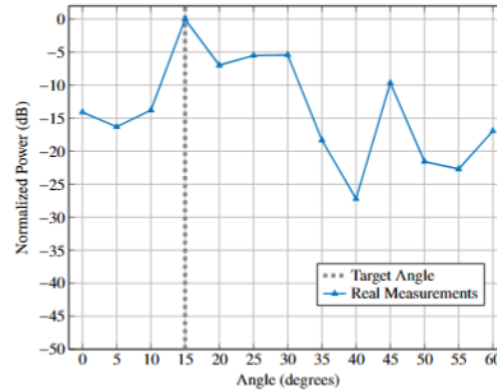
## 1-bit RIS

- Blue → 0 state
- Yellow → 1 state

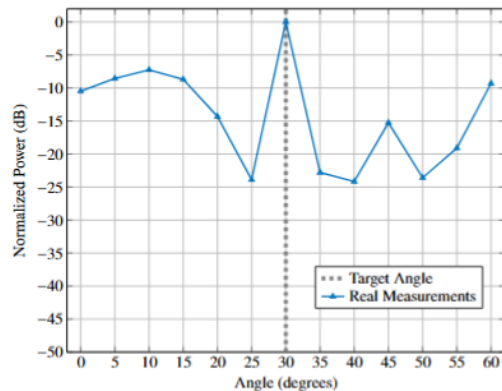
# Measured Radiation Patterns of RIS (Codebook)



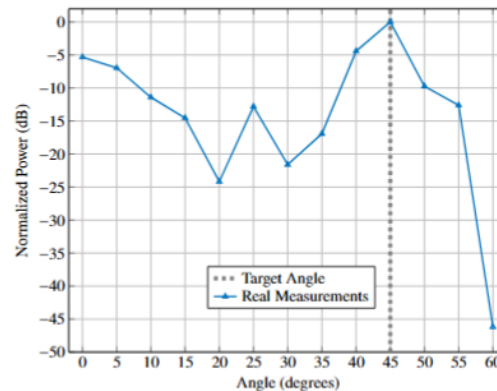
(a) Beam at 0°



(b) Beam at 15°



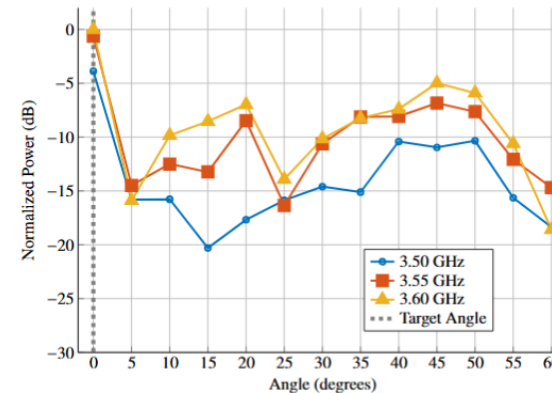
(c) Beam at 30°



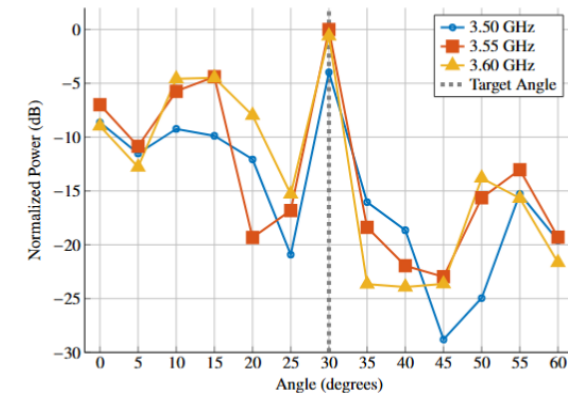
(d) Beam at 45°

Outdoor measurements

- ✓ All setups have been evaluated (indoor, outdoor, anechoic chamber)
- ✓ Maximum received signal power is measured at the receiver position aligned with the intended beam steering direction



(a) Beam at 0°



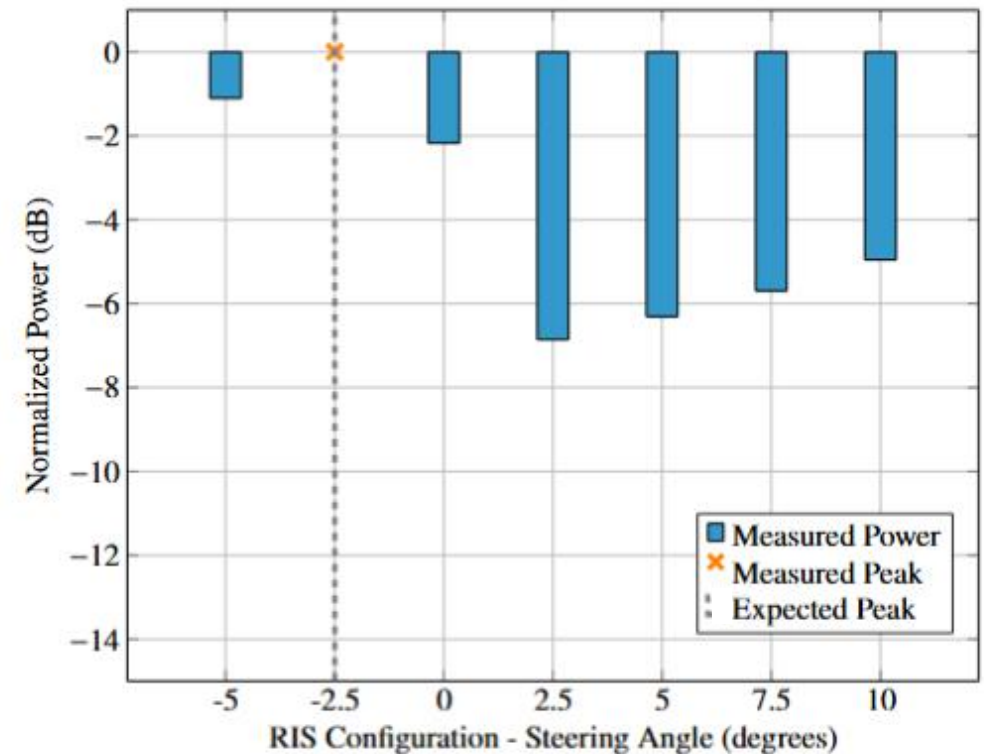
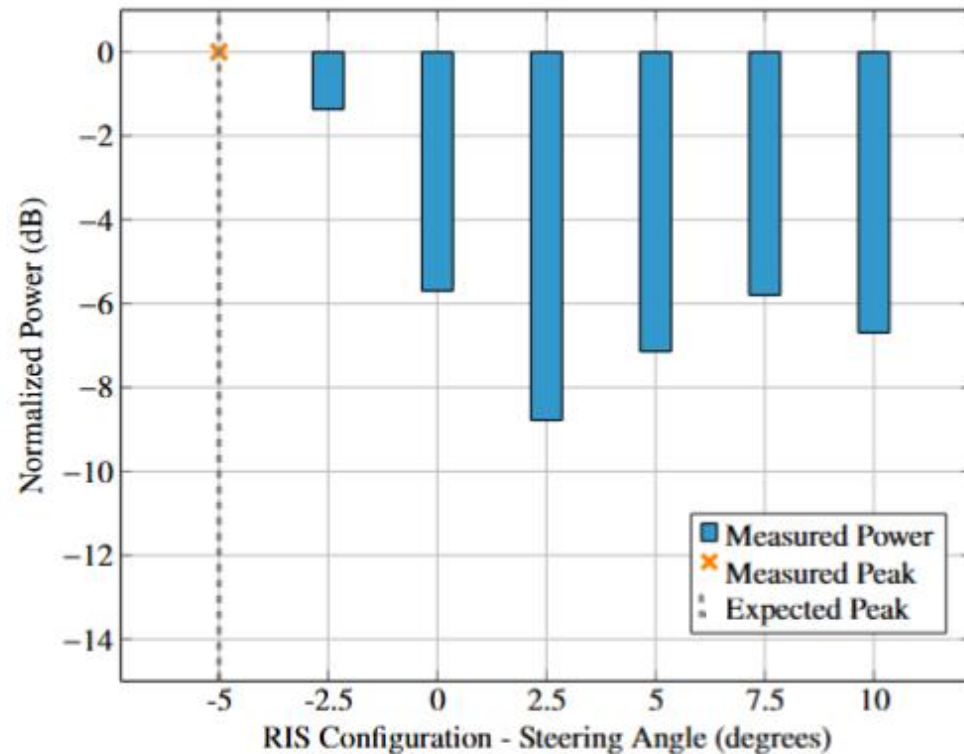
(b) Beam at 30°

## Frequency selectivity of RIS Radiation Patterns:

- Angle direction of the main lobe is preserved across the frequency range
- Variations are observed in the side lobes

# Anechoic Chamber: AoA Estimation via Beam Sweeping

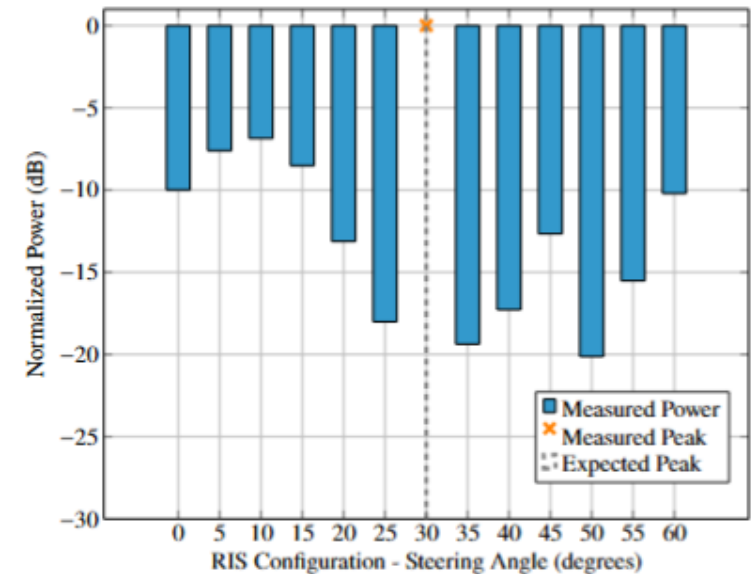
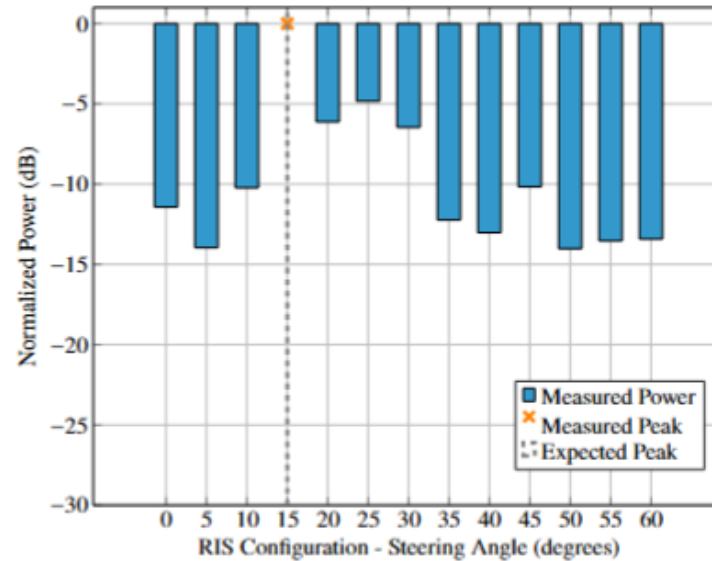
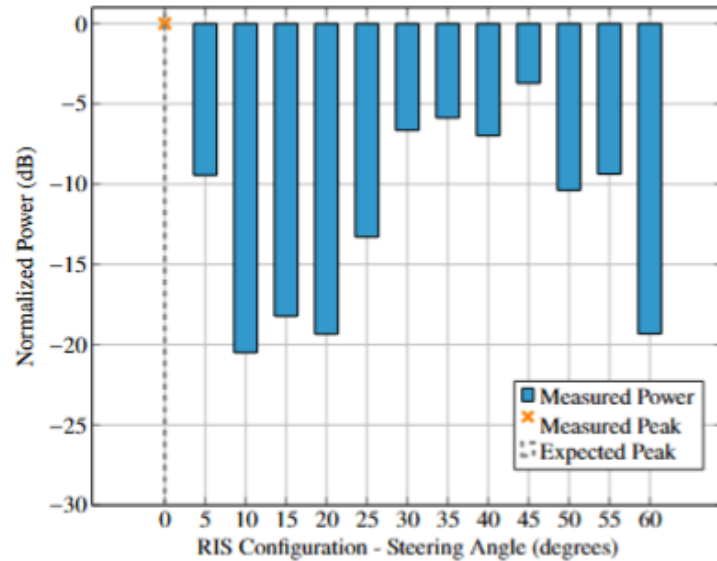
- Reflection-free environment, limited space
- **Expected peak:** RIS-Rx azimuth angle
- **Measured peak:** angle for which the strongest received signal was observed





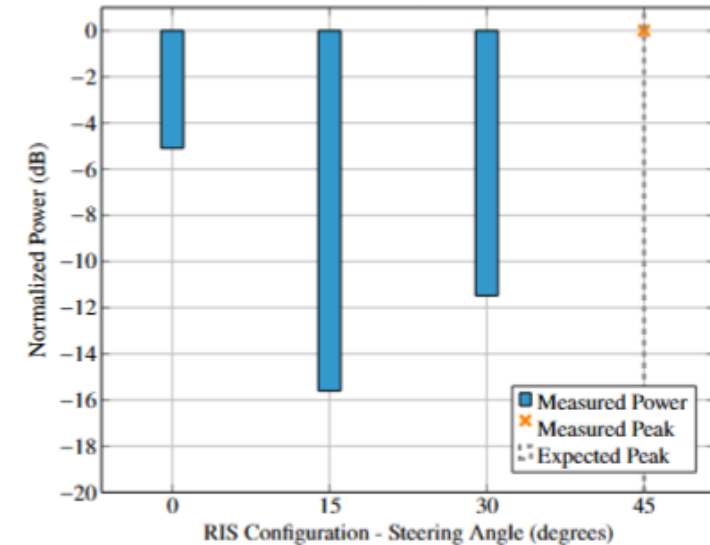
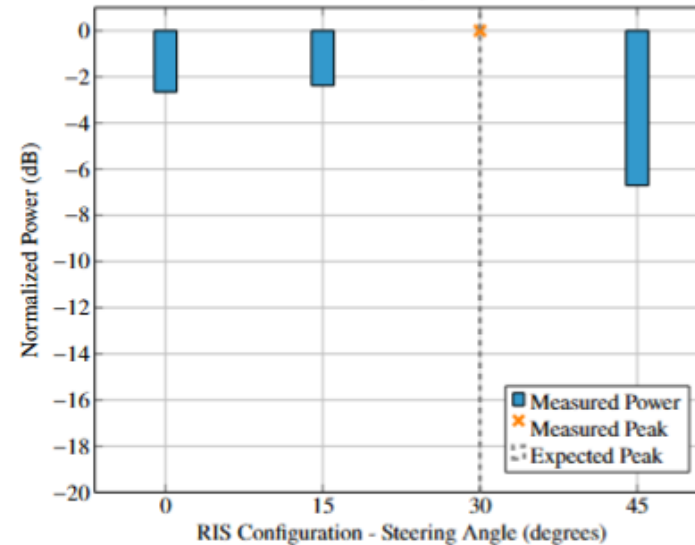
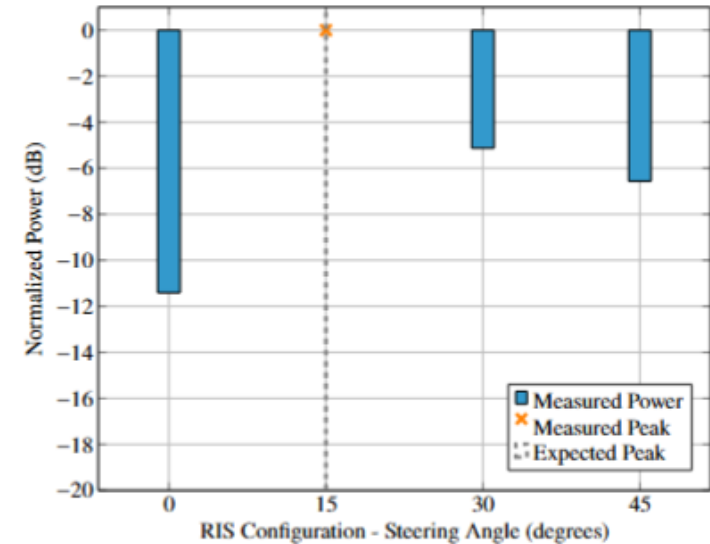
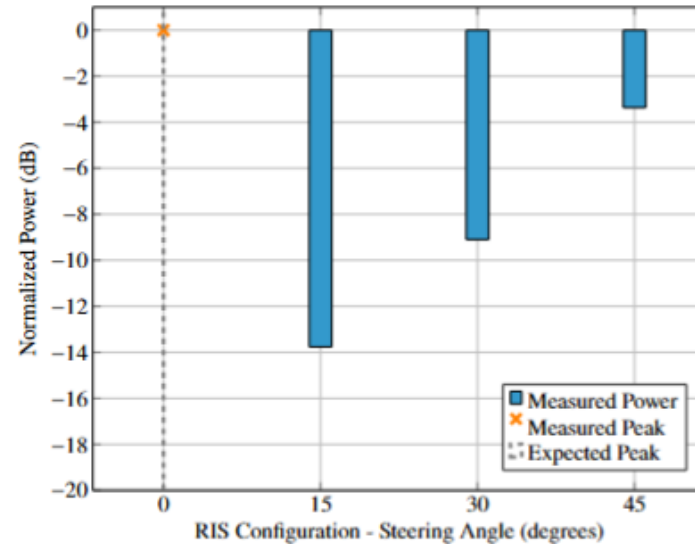
# Outdoor Setup: AoA Estimation via Beam Sweeping

- Limited multipath
- **Expected peak:** RIS-Rx azimuth angle
- **Measured peak:** angle for which the strongest received signal was observed



# Indoor Setup: AoA Estimation via Beam Sweeping

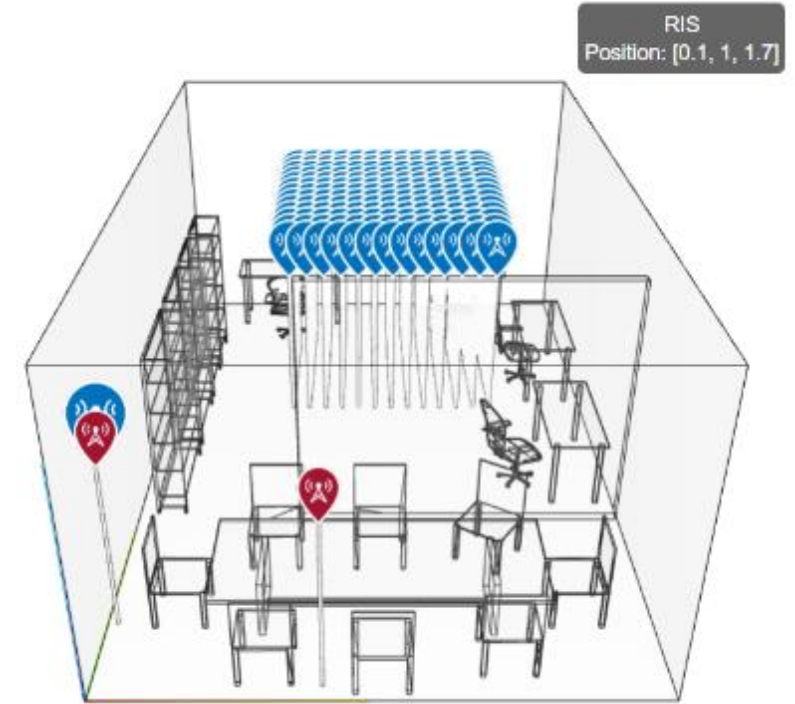
- Strong multipath
- **Expected peak:** RIS-Rx azimuth angle
- **Measured peak:** angle for which the strongest received signal was observed



# RIS-Aided Angle of Arrival Estimation

## General Idea for RIS-Assisted Positioning

- RIS helps super-resolution algorithms accurately calculate the AoA of the LoS path by strengthening it over other paths.
  - Seek a RIS configuration that beamforms towards the LoS path.
- Design an offline codebook of RIS configurations.
  - The UE position is not known to directly beamform to it using the RIS!
- Select the RIS configuration that maximizes UE's received power before estimating AoA.



Phase shifters	RIS configuration	Method	Peak	Average	Variance
Continuous	$\omega_\theta^T$	BeS <sup>†</sup>	12.62°	1.03°	2.28°
1-bit RIS	Quantized $\omega_\theta$	BeS	58.28°	9.93°	280.32°
1-bit RIS	Quantized $\omega_\theta$	BeS & MUSIC	10.68°	0.86°	1.82°

<sup>†</sup> BeS: Beam Sweeping

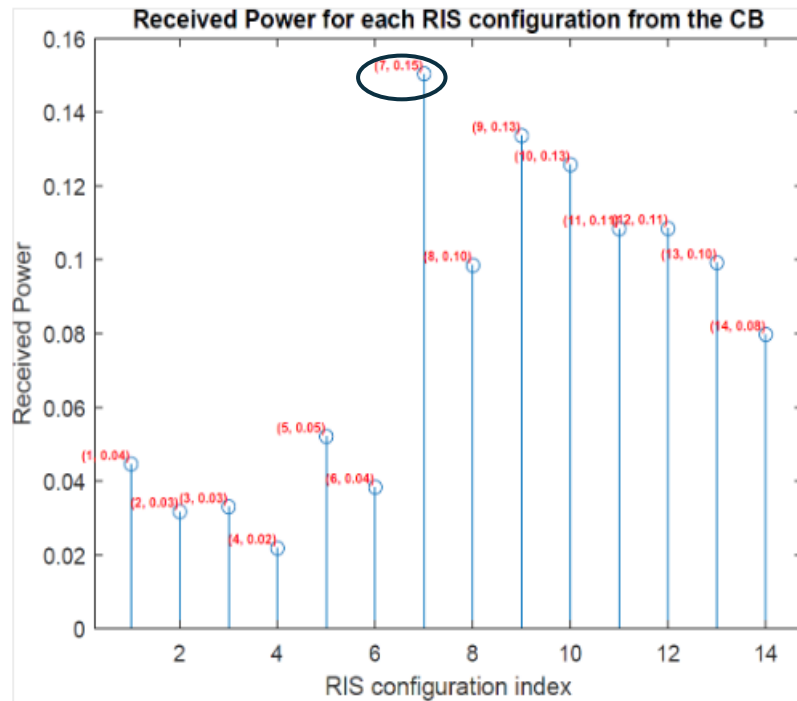
## Ray Tracing Simulation Results

- Beam sweeping struggles in 1-bit RIS systems under strong multipath conditions, since side lobe effects activate unintended NLoS paths.
- MUSIC achieves robust and precise positioning, comparable to the scenario where a continuous RIS is employed.

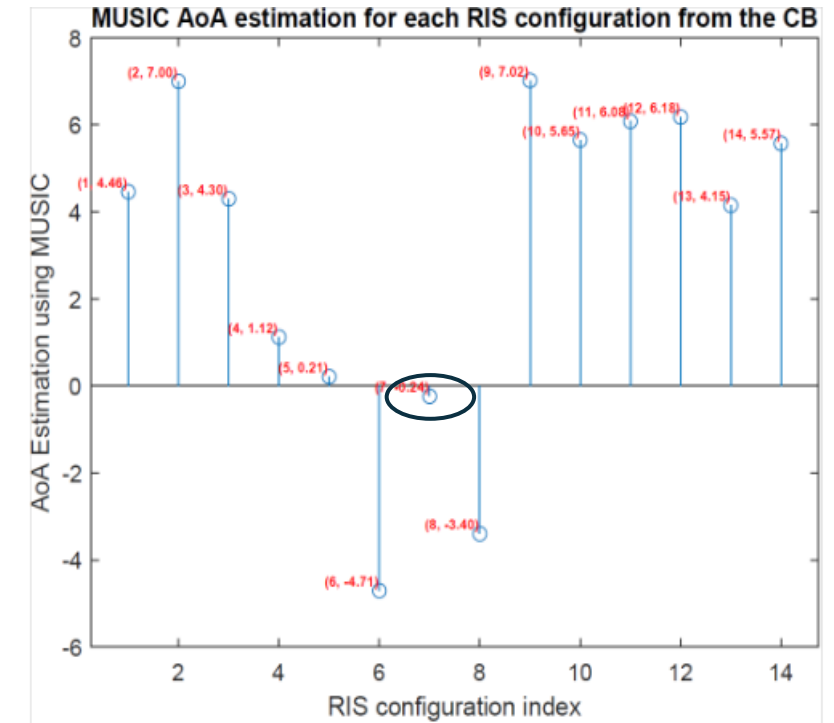
# RIS-Aided AoA Experimental Results

## Setup1: Anechoic Chamber

- Tx at  $-15^\circ$ , RX at  $2.5^\circ$
- All nodes are placed at the same height
- $2 \times 7 = 14$  RIS configurations (reflecting at  $-5^\circ$  to  $10^\circ$  with step of  $2.5^\circ$ )
- 2 RIS configurations for each position, corresponding to 2 iterations of greedy algorithm
- Three-antenna ULA is directed towards the RIS center



Beam Sweeping results when RX is located at  $2.5^\circ$ . RIS configurations 7 and 8 are optimized for RX at  $2.5^\circ$ . Also RIS-configuration 7 wins at the Beam Sweeping.



MUSIC results when RX is located at  $2.5^\circ$ . RIS configurations 7 and 8 are optimized for RX at  $2.5^\circ$ . Also RIS-configuration 7 wins at the Beam Sweeping.





Photos: PRISM indoor setups ECE Dept., UPAT

## RIS-Aided AoA Experimental Results

### Setup2: Indoor Environment

- Tx at  $-15^\circ$
- 4 RIS configurations (reflecting at  $0^\circ$  to  $45^\circ$  with step of  $15^\circ$ )
- Three-antenna ULA is directed towards the RIS center



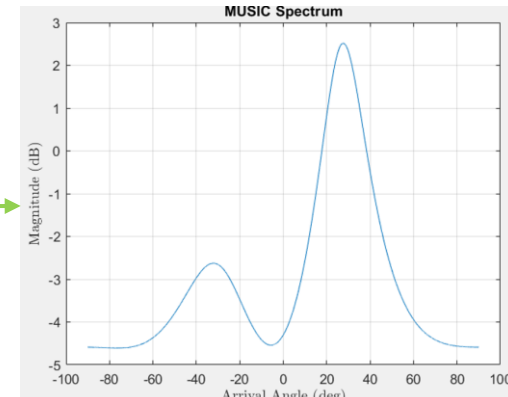
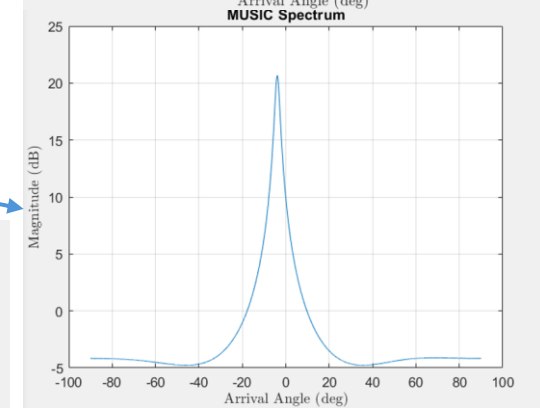
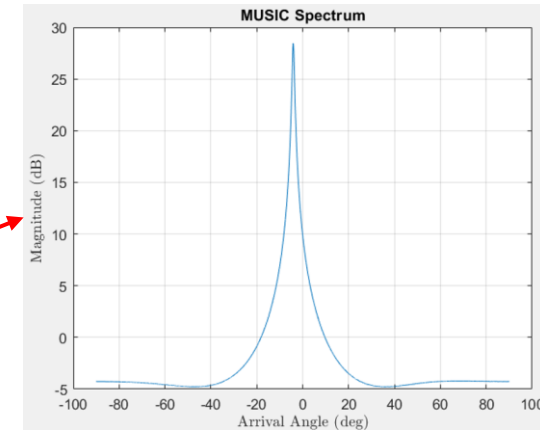
# RIS-Aided AoA Experimental Results and Measurements

## Setup2: Indoor Environment

- Tx at  $-15^\circ$
- 4 RIS configurations (reflecting at  $0^\circ - 45^\circ$  with step of  $15^\circ$ )
- Three-antenna ULA is directed towards the RIS center

Results of the RIS-aided AoA estimation for various Tx signals, and with different Tx/Rx gains.

Setup	TX signal	TX gain (dB)	RX gain (dB)	Ground Truth AoA ( $^\circ$ )	AoA estimation ( $^\circ$ )
'right'	SINE	15 dB	25 dB	$0^\circ$	$-3.9^\circ$
'right'	SINE	15 dB	30 dB	$0^\circ$	$-4.1^\circ$
'right'	SINE	20 dB	25 dB	$0^\circ$	$-4.54^\circ$
'right'	SINE	25 dB	25 dB	$0^\circ$	$-4.28^\circ$
'right'	PRS	15 dB	25 dB	$0^\circ$	$-7.28^\circ$
'right'	PRS	15 dB	30 dB	$0^\circ$	$-3.56^\circ$
'left'	PRS	15 dB	30 dB	$0^\circ$	$1.02^\circ$
'left'	PRS	15 dB	30 dB	$25^\circ$	$27.35^\circ$



**Conclusion: Even in challenging indoor environments, an average angle estimation error of  $\approx 5^\circ$  can be achieved.**

# RIS-Aided Ranging Experimental Setup

**Goal:** Estimate the TDoA between two dominant paths

- Cross-correlation between the RX and the known TX signal
- Error depends on the sampling period
- $F_s = 153.6$  MHz



Photo: PRISM indoor setup ECE Dept., UPAT

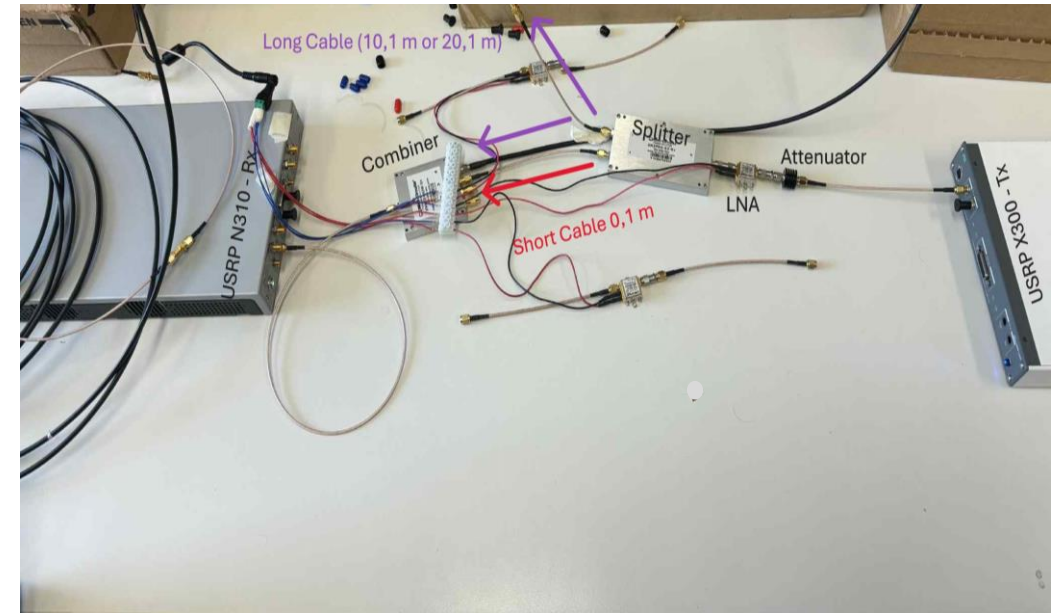
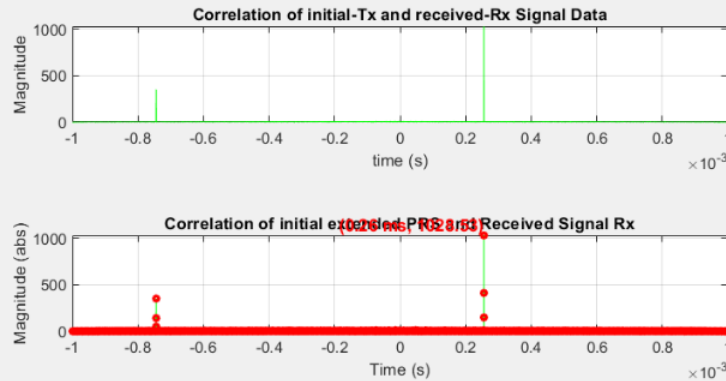


Photo: PRISM setup at VLSILAB, ECE Dept., UPAT

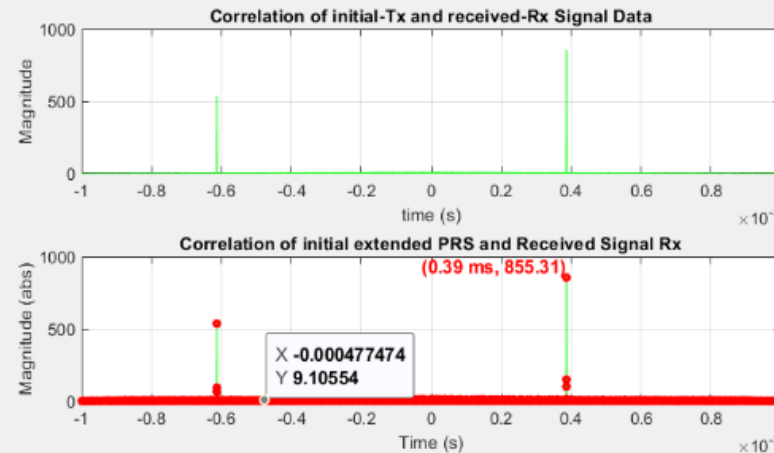
# RIS-Aided Ranging Experimental Results

10 m cable length dif.

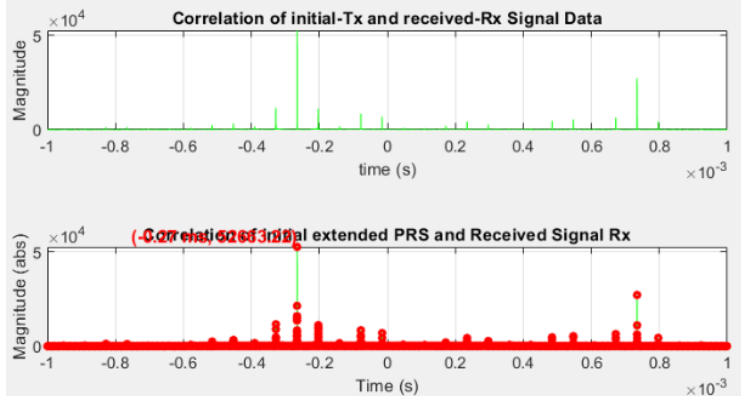


- Length Distance Estimation is 9.72 m
- Using Interpolation Parabola: 9.91 m

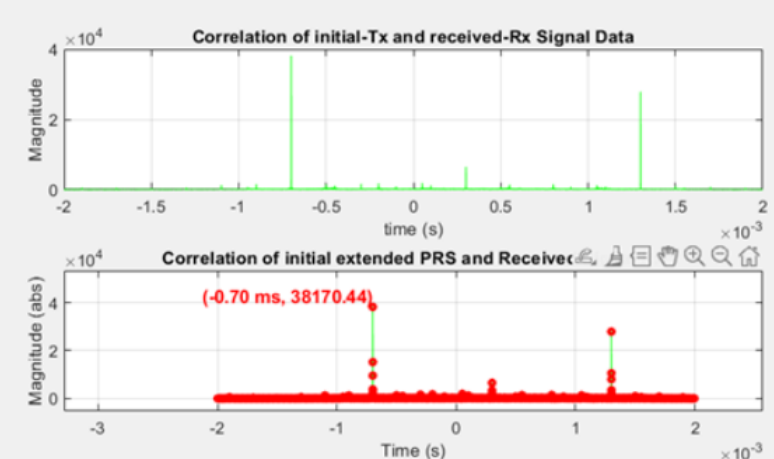
20 m cable length dif.



- Length Distance Estimation is 19.44 m
- Using Interpolation Parabola: 19.67 m

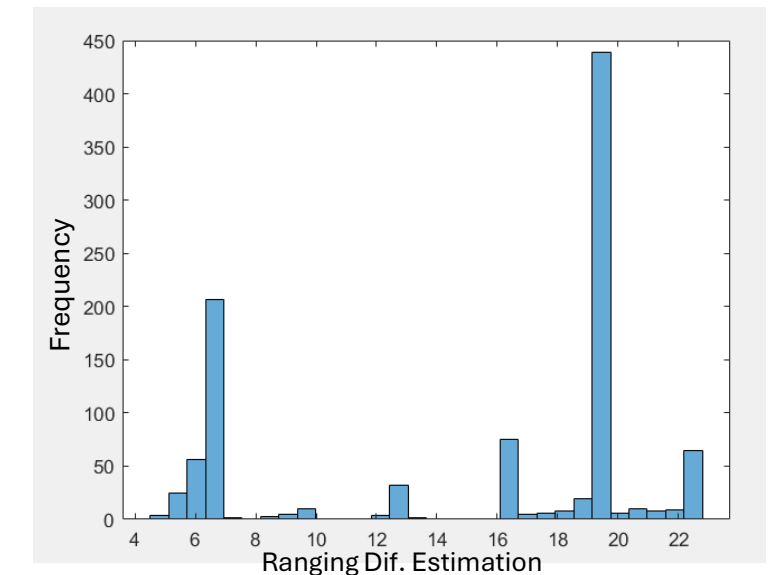


- Length Distance Estimation is 11.33 m
- Using Interpolation Parabola: 11.91 m



- Length Distance Estimation is 19.43 m
- Using Interpolation Parabola: 19.53 m

- Variations due to pathloss in 20m case
- RIS more accurate and enhanced beamforming is required.



# RIS-Aided Mapping: Methodology

## Objective:

- Localize a passive scatterer by exploiting RIS-induced RF fingerprints

## Setup:

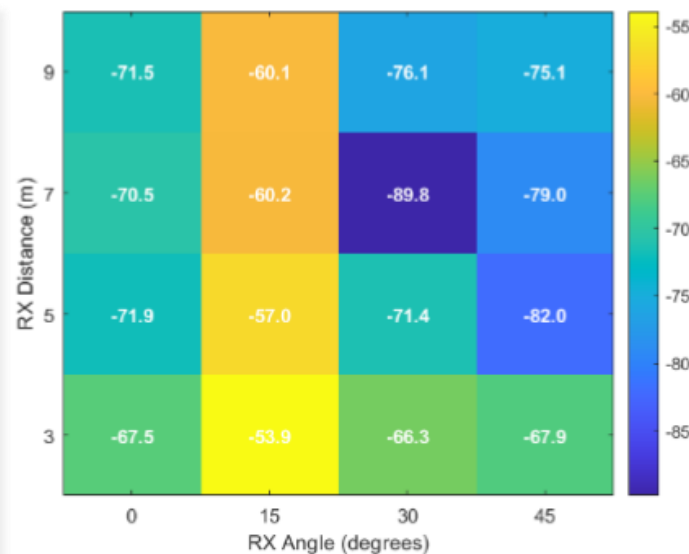
- Indoor environment with ITELITE directional antennas for Tx/Rx
- Tx fixed at azimuth  $-15^\circ$  relative to RIS
- Scatterer at  $-30^\circ$  (Tx-RIS path),  $+30^\circ$  (RIS-Rx path), placed 2m away from the RIS

## Measurement protocol:

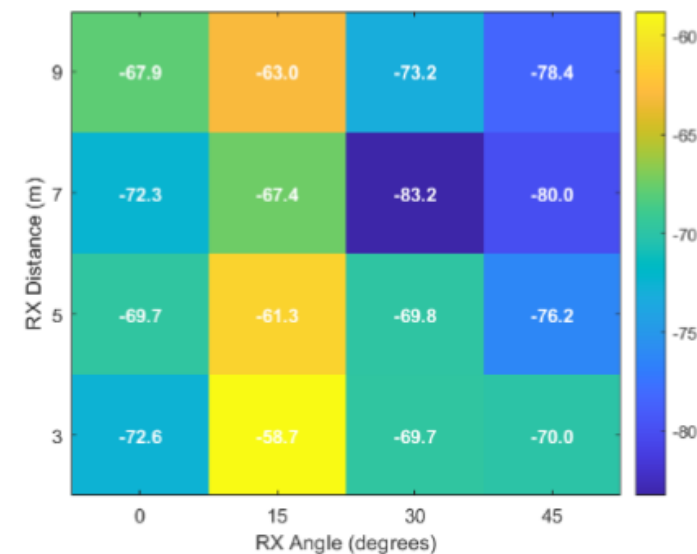
- Baseline heatmap created by moving RX over a 2D grid and recording power for a set of RIS configurations (both random and optimized configurations).
- Scatterer introduced; process repeated to generate a second heatmap.
- Differential analysis of the two maps reveals scatterer position (angle & distance).

# RIS-Aided Mapping: Experimental Results

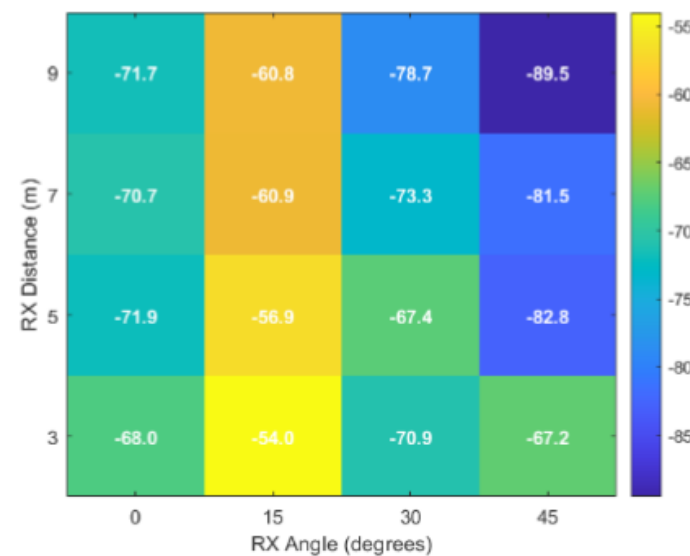
- Scatterer at  $-30^\circ$  (Tx–RIS path):  
Entire map affected  $\rightarrow$  obstructions on main illumination path detected regardless of RX position
- Scatterer at  $+30^\circ$  (RIS–Rx path):  
Consistent changes along  $30^\circ$  RX column  $\rightarrow$  Correct azimuth identification and coarse distance estimation of the scatterer ( $<3$  m)



(a) Baseline (no scatterer)



(b) Scatterer at  $-30^\circ$



(c) Scatterer at  $+30^\circ$



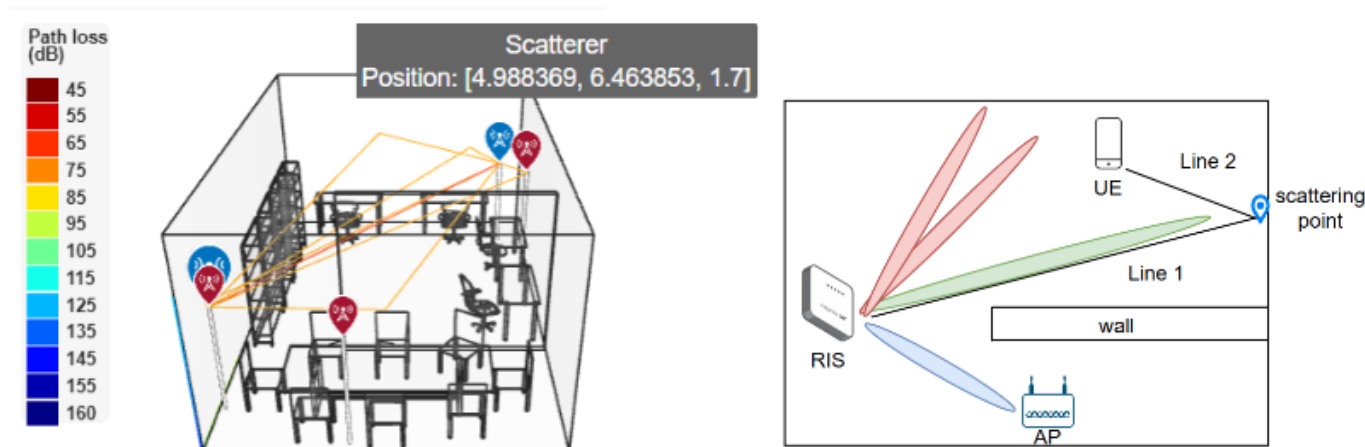
# RIS-Aided Mapping

## Objective: Specifying the Location of Scattering Points

- NLoS paths of a single reflection point are resolved.
- Since ULA-based UEs are used, only NLoS paths without elevation can be resolved.

## Algorithmic Solution

- Estimate the position of the UE (LoS-path's parameters).
- Compute the RIS-to-UE LoS channel.
- Generate the estimated LoS-term part of the RX signal.
- Subtract the LoS term from the RX signal.
- Execute Beam Scanning.
- When RIS targets at an NLoS path, the angle found by MUSIC is that of scatterer-to-UE.
- The location of the scattering point is specified as the intersection of two straight lines.



Path Number	Path Type	Azimuth AoA	Elevation AoA (deg, °)
1.	LoS	53.75°	0
2.	NLoS	127.36°	$8.56 \times 10^{-14}$
3.	NLoS	53.75°	21.96
4.	NLoS	47.91°	0
5.	NLoS	53.75°	-24.56
6.	NLoS	61.29°	0

The RIS-enabled approach achieves an average scattering point estimation error of 0.21 m

# Conclusions

---

- **RIS Characterization and Experimental Setups**
  - Identification of beamforming limitations overlooked in theoretical studies
  - Field trials in diverse environments (indoor, outdoor, anechoic chamber)
  - Development of model-free methods for localization & mapping
- **Angle Estimation**
  - Proposed super resolution estimation combined with RIS beam sweeping proven effective
  - 1° average error in simulations; 4°- 10° average error in indoor experimental setups
  - Discrepancies between simulations and experiments due to actual hardware behavior, radiation pattern and channel modeling
- **Range Estimation and Mapping**
  - Fingerprinting methods proven valuable in experimental setups
  - Proposed RIS-based techniques show potential in simulations

# Demo

